Beta-caryophyllene enhances wound healing through multiple routes

(65 characters)

Short title: Beta-caryophyllene and wound healing

Sachiko Koyama[1*], Anna Purk[2], Manpreet Kaur[3], Helena A. Soini[4], Milos V. Novotny[4], Keith Davis[1], C. Cheng Kao[5], Hiroaki Matsunami[6], Anthony Mescher[7]

Affiliations

[1]Department of Biology, Biotechnology Program, Indiana University, Bloomington, IN, USA.

[2]School of Public Health, Indiana University, Bloomington, IN, USA

[3]Department of Psychological and Brain Sciences, Indiana University, Bloomington, Indiana, USA

[4]Department of Chemistry, and Institute for Pheromone Research, Indiana University, Bloomington, Indiana, USA

[5]Department of Molecular and Cellular Biochemistry, Indiana University, Bloomington, Indiana, USA

[6]Department of Molecular Genetics and Microbiology, School of Medicine, Duke University, Durham, North Carolina, USA

[7]Department of Anatomy and Cell Biology, School of Medicine, Indiana University, Bloomington, Indiana, USA

* Correspondence author

E-mail: apodemusmice@gmail.com

Abstract

Beta-caryophyllene is an odoriferous bicyclic sesquiterpene found in various herbs and spices. Recently, it was found that beta-caryophyllene is a ligand of the cannabinoid receptor 2 (CB2). Activation of CB2 will decrease pain, a major signal for inflammatory responses. We hypothesized that beta-caryophyllene can affect wound healing by decreasing inflammation. Here we show that cutaneous wounds of mice treated with beta-caryophyllene had enhanced re-epithelialization. The treated tissue showed increased cell proliferation and cells treated with beta-caryophyllene showed enhanced cell migration, suggesting that the higher re-epithelialization is due to enhanced cell proliferation and cell migration. The treated tissues also had up-regulated gene expression for hair follicle bulge stem cells. Olfactory receptors were not involved in the enhanced wound healing. Transient Receptor Potential channel genes were up-regulated in the injured skin exposed to beta-caryophyllene. Interestingly, there were sex differences in the impact of beta-caryophyllene as only the injured skin of female mice had enhanced re-epithelialization after exposure to beta-caryophyllene. Our study suggests that chemical compounds included in essential oils have the capability to improve wound healing, an effect generated by synergetic impacts of multiple pathways. (184 words)

Introduction

Odors from other conspecific[1] individuals [1] and the environment [2-6] affect the behaviors and physiological status in many animals. The significance of olfactory stimuli tends to be underestimated in case of humans. However, we have a long history of actively utilizing odorants to heal or alter our physiological conditions. Various herbal plants' and spices' extracts have been used to reduce stress, pain, and to promote recovery from injury or illness [2-6]. In spite of such a long history of using herbal plant extracts and although an increasing number of scientists are starting to test natural products owing to their diverse molecular scaffolds and biologically active substructures, there is still a strong need to examine the influences of extracts. It is especially important to better understand their mechanisms of action.

When essential oils are used instead of single chemical compound, there have been challenges to examine their mechanism of action because of the large variances in the percentage each chemical compound present [7] depending on the extraction methods [8], the area of origin including differences in the geographic altitude of the areas [9], seasons the plants were harvested [10], and parts of the plants extracted [11,12]. It is thus important to utilize chemically-pure compounds or chemically-defined extracts as described in some recent studies [13-17]. These studies enable testing the roles of individual chemicals and obtaining clear mechanistic insights [13,14].

In addition, the route of administration can affect the efficacy of the odorants. Odorants of herbal plants are often called "aromas", which suggests that the route is through the olfactory system. However, there are various routes that odorant chemicals can exert

[1] Conspecific: Technical terms in the study field of animal behavior and ethology, meaning the same species

effects. First, olfactory receptors are expressed in both olfactory neurons and in non-olfactory tissues, such as skin and circulatory organs [18,19]. Furthermore, some odorants activate both olfactory receptors and non-olfactory receptors. For example, beta-caryophyllene (BCP), which is an odoriferous bicyclic sesquiterpene present in many herbs and spices, is a ligand of cannabinoid receptor 2 (CB2)[2] [20] as well as olfactory receptors. How odorants such as BCP act on distinct receptor classes is important for the most effective use of BCP.

The CB2 receptor is expressed in neuronal cells, immune tissue, hair follicles, sebaceous glands, the dermomuscular layer, and vascular smooth muscle in intact skin [21]. Activation of CB2 by CB2 selective agonist GP1a improved re-epithelialization in wound healing [22,23]. Essential oil of *Copaifera paupera,* which contains BCP also improved wound healing [24], although it is not clear whether BCP had a direct or indirect role and whether the wound healing is promoted by the CB2 receptor. In this project, we examined whether BCP can improve re-epithelialization and, if so, whether the olfactory system is involved in the impact.

Results and discussion

BCP treatment enhanced re-epithelialization

Wound healing is a series of overlapping cellular and biochemical processes that restore the integrity of injured tissues. In general, healing occurs with four overlapping

[2] Cannabinoid receptors G-protein receptors first found as the receptors for Δ^9-tetrahydrocannabinol (THC), which is the main psychoactive constituent of *Cannabis sativa* (marijuana). Two receptors have been identified, cannabinoid receptors 1 and 2 (Zou S, Kumar, U. *Int. J. Mol. Sci*, 2018, 19, 833).

84 phases that takes place from minutes to weeks: hemostasis, inflammation, cell proliferation
85 and migration, and maturation/scarring [25-28]. We examined whether exposure to BCP
86 affect cell proliferation and the re-epithelialization of mouse skin in a full thickness wound
87 generated on the back of mice using scissors. The wound was then covered with a device
88 that can retain either 50 uL of BCP (50mg/kgbw, diluted with olive oil) or a control (olive
89 oil alone) (see Materials and Methods for details, S1 Fig). Throughout the study, none of the
90 mice exhibited behaviors suggestive of irritation with the BCP (S2, S3 Fig).
91 Immunofluorescence staining of keratin-14 (K14), a marker of re-epithelialization [29],
92 revealed that wounds treated with BCP had increased keratinocyte migration distance
93 from intact skin near the wound toward the wound center relative to the controls,
94 indicating improved re-epithelialization (Fig. 1). Staining for proliferating cell nuclear
95 antigen (PCNA) showed that many cells were proliferating at the wound edge in both the
96 BCP and Oil groups (green color in the wound edge area in Fig. 1b). In the BCP group,
97 PCNA+ fibroblast cells are concentrated in the reticular dermis (lower area of dermis). The
98 fibroblast cells in the reticular dermis migrate into the wound bed and form an
99 extracellular matrix of granulation tissue [30]. The results on K14 and PCNA show that the
100 BCP-treated group exhibits higher re-epithelialization and cell proliferation.
101 Another marker of re-epithelialization is the expression of filaggrin, a marker of
102 differentiated skin [31]. Filaggrin is expressed in the upper layer of the epidermis (stratum
103 corneum) and functions as a skin barrier, protecting the body from losing water and from
104 exogenous pathogens [31]. In the BCP-treated wounds, the range of differentiated stratum
105 corneum layer in the invading epidermis was wider and the expansion from the wound
106 edge was longer when compared to the Oil group (Fig. 2 red).

107 Estrogen is known to accelerate wound healing [32]. We examined if there are
108 differences in the expression of estrogen receptor alpha after exposure to BCP. Estrogen
109 receptor alpha was expressed strongly in the dermis fibroblasts of both the BCP and Oil
110 group without differences (Fig. 2).
111 Platelet-derived growth factor-A and –B (PDGF-A and –B) are expressed in fibroblasts
112 and keratinocytes [33]. PDGF receptors (PDGFR) are expressed in fibroblasts, smooth
113 muscle cells, epithelial cells, macrophages, and their expression increases when there is
114 inflammation [33]. In wound healing, PDGF stimulates mitogenesis and chemotaxis of
115 fibroblasts, smooth muscle cells, neutrophils and macrophages, and stimulates production
116 of fibronectin, collagen, proteoglycans and hyaluronic acid [33]. PDGFRα also has a role in
117 both extracellular matrix and hepatocyte growth factor production in fibroblasts in
118 remodeling of connective tissue [34]. Immunofluorescence staining for PDGFRα showed
119 that it is expressed strongly in the epidermis and the wound edge of the tissue treated with
120 BCP (Fig. 2b). In the tissues treated with Oil, PDGFRα was expressed strongly only at the
121 wound edge (Fig. 2b). Vimentin, which has a role in fibroblast proliferation and
122 keratinocyte differentiation [35,36], was expressed strongly in the wound edge (Fig. 2b
123 red) of both the BCP-treated and Oil-treated wound. These results suggest that the impact
124 of BCP is primarily on the invasion of epidermis and differentiation of keratinocytes,
125 resulting in enhance re-epithelialization of the wounded area.
126
127 **Fig 1. Re-epithelialization measured by keratin 14. (a)** Immunofluorescence staining of
128 K14 (red) and PCNA (green) with nuclear staining using Draq5 (blue) of skin with wound
129 treated with BCP or with oil. **(b)** Higher magnification images of areas of boxes in **(a)**.

130 PCNA was localized in the nucleus and, when density of cells increased, it became localized
131 in the cytoplasm **(b)**. This was observed at the center of the wound. In: intact area, W:
132 wounded area. **(c, d)** Length of K14+ staining area from the boundary of intact and
133 wounded area to the center of the wound in skin harvested on post-surgery day 3 **(c)** and 4
134 **(d)**. Dots indicate each datum and the height of bars indicates the median. Horizontal lines
135 indicate quartiles. 3rd day, Kolmogorov-Smirnov test, P=0.008, BCP, n=20, Oil, n=15; 4th day,
136 Kolmogorov-Smirnov test, P=0.002, *: P<0.05, BCP, n=16, Oil, n=16. (142 words)
137
138
139 **Fig. 2 Expression of filaggrin (red) and estrogen alpha (green) (a), and PDGFR**
140 **(green) and vimentin (red) (b) in the wounded area of mice. (a)** View at the wound
141 edge. In: intact area, WE: wound edge, WB: wound bed. Scale bar is in μm. Dotted lines
142 show the boundaries between the intact area and wound edge, and the wound edge and
143 wound bed. Filaggrin staining of the BCP group was broader in width and longer in the
144 distance from the wound edge. Estrogen alpha staining did not show obvious differences
145 between groups. **(b)** PDGFR expression in the epidermis was stronger in the BCP group.
146 Both the BCP and Oil group showed a large area of staining of PDGFR in the wound edge
147 (WE) and wound bed (WB). Vementin staining did not show obvious differences between
148 the BCP group and Oil group. In: intact area, WE: wound edge, WB: wound bed. Scale bars
149 are in μm. (153 words)
150

151 **BCP treatment enhanced cell proliferation**

152 To determine the rate and location of cell proliferation in the wounded tissue, 5-bromo-
153 2'-deoxyuridine (BrdU) was injected twice every 2 hours and tissues were harvested 2
154 hours after the second injection (see Materials andMethods for details). Significantly more
155 BrdU+ cells were found on the basal layer of the interfollicular epidermis and hair follicles,
156 and in the papillary dermis [37-39] in the BCP-treated wounds. In both the BCP-treated
157 and controls, there were many BrdU+ cells at the wound margin and wound bed (Fig. 3).
158 Previous studies have shown that proliferation takes place at a proliferative hub, which is
159 from 2 mm outside of the wound edge until 3 mm from the wound edge [40]. We observed
160 that cell proliferation in the controls took place highly at the wound margin and at the basal
161 layer of the interfollicular epidermis (Fig. 3f, Oil). In contrast, the BCP-treated wounds had
162 higher cell proliferation in the interfollicular epidermis, in the dermis, at the hair follicles,
163 and in the wound bed (Fig. 3f, BCP).
164 Stem cells in the hair follicle contribute to re-epithelialization by migrating from the
165 hair follicle bulge to epidermis and then to the center of the wound [41]. The strong BrdU
166 staining of hair follicles in the BCP-treated wounds compared to the controls suggest that a
167 larger number of hair follicle stem cells may have contributed to the enhanced re-
168 epithelialization in BCP group.
169
170 **Fig 3. BrdU+ cells in the epidermis and dermis. (a)** BrdU+ cells in the epidermis (epi in
171 **(f)**) (Student T-test, T=3.077, df=8, *P*=0.015, BCP, n=5, Oil, n=5), **(b)** BrdU+ cells in the
172 wound margin (wm in **(f)**) (Student T-test, T=1.343, df=8, *P*=0.216, BCP, n=5, Oil, n=5), **(C)**
173 BrdU+ cells at the hair follicle (h in **(f)**) (Student T-test, T= 3.038, df=8, *P*=0.015, BCP, n=5,
174 Oil, n=5). **(d)** BrdU+ cells at the dermis excluding wound margin (Student T-test, T=4.645,

175 df=8, *P*=0.002, BCP, n=5, Oil, n=5). **(e)** BrdU+ cells at the BrdU+ cells at the wound bed
176 (Student T-test, T=2.197, df=8, *P*=0.059, BCP, n=5, Oil, n=5). **(f)** Representative views of
177 combined photos used in quantification for each group. h: hair follicle, epi: epidermis, der:
178 dermis, wm: wound margin, wb: wound bed, scale bar: 200 μm. Numbers below and above
179 the photos are operationally assigned numbers for explanation in the text on locations in
180 the wound. Dotted lines show the boundaries between epidermis and dermis, dermis and
181 wound margin zone, and wound margin zone and wound bed. (172 words)
182
183 If enhanced re-epithelialization was due to a reduction of inflammation and an early
184 shift to the cell proliferation/migration stage, then BCP should not impact cultured cells.
185 To test this hypothesis, we conducted time-lapse imaging for 7 hours and enumerated cell
186 division. We conducted this with different concentrations of BCP. We found a peak of cell
187 proliferation at 26 μM BCP, which decreased at higher concentrations (Fig. 4). In higher
188 concentrations we observed less cell proliferation. These results suggested that BCP
189 treatment was on cell proliferation and enhanced re-epithelialization rather than the
190 suppression of inflammation.
191
192 **Fig 4. Proliferating primary fibroblast cells exposed to BCP at various**
193 **concentrations.** Number of dividing and apoptotic cells during 7 hours of exposure to BCP.
194 (23 words)
195

196 # BCP enhanced cell migration

197 The increased cell migration caused by BCP was not reported previously and we
198 examined this further. To determine whether exposure to BCP can stimulate cell
199 migration, we conducted *in vitro* assays of scratch tests and chemotaxis assays. Primary
200 cultured fibroblasts and keratinocytes from C57BL/6 mice exposed to BCP (diluted with
201 DMSO) for 24 hours showed higher chemotactic responses relative to the controls
202 (fibroblasts, 2.1 times higher number of cells, and keratinocytes, 2.5 times higher number
203 of cells, both compared to control condition cells exposed to DMSO) (Fig. 5a, b, c).
204 However, exposure to BCP did not stimulate chemotactic responses in fibroblasts isolated
205 from CB2 knockout mice (1.2 times higher number of cells compared to control condition
206 cells exposed to DMSO) (Fig. 5d). These results suggest that activation of CB2 could lead to
207 an increase in chemotactic responses.
208
209 **Fig 5. Influence of BCP on cell migration. (a)** Representative results of chemotaxis assay.
210 Cells showed chemotactic responses to BCP. Fibroblasts and keratinocytes were exposed
211 either to BCP or to DMSO (control) in chemotaxis assay. WT cells exposed to BCP showed
212 significantly more chemotactic responses toward the bottom of the inserts (fibroblasts,
213 Student T-test, T=2.564, df=8, *P*=0.033, BCP, n=4, DMSO, n=4, **(b)**; keratinocytes, Student T-
214 test, T=2.456, df=8, *P*=0.04, BCP, n=4, DMSO, n=4, **(c)**), but cells isolated from CB2 knockout
215 mice did not show differences between those exposed to BCP and those exposed to DMSO
216 control (fibroblasts, Student T-test, T=0.944, df=4, *P*=0.398, BCP, n=3, DMSO, n=3, **(d)**). **(e,**
217 **f, g)** Results of scratch tests. Representative images on the influence of BCP (27 μM) on cell
218 migration of fibroblasts. Six hours after scratch **(e)** and 1 day after scratch **(f)**. Dotted
219 white lines show the edge of scratched area. Scale bar = μm, **(g)** The distance cells migrated

220 during the 6 hours shown as a comparison to the original width (% of shrink in width).
221 0% means no change from original width. ANOVA, Medium type, $F_{1,8}$=7.16, P=0.028, cell
222 type, $F_{1,8}$=0.365, P=0.562, BCP, n=3, DMSO, n=3. (192 words)
223
224 In the chemotaxis assay above we found that cells show chemotactic responses toward
225 BCP. We then conducted scratch tests to determine if exposure to BCP stimulates
226 chemotactic responses to repopulate in petri dishes. After culture dish reached confluency,
227 the culture media was replaced to culture media containing BCP (23μM/10 μL DMSO/10
228 mL cell culture media) or DMSO (10 μL/10mL cell culture media). Exposure to BCP
229 increased cell migration to the scratched area (39.2% decrease in the width in 6 hours),
230 relative to the control (6.7% decrease in the width in 6 hours). The cells from CB2
231 knockout mice exposed to BCP also showed a comparable rate of repopulating the
232 devoided area (34.0% decrease in the width in 6 hours) (Fig. 5e, f, g). These results suggest
233 that BCP can stimulate cell migration, but not through CB2 pathway.
234 We started this study with the hypothesis that BCP will positively impact wound
235 healing by activating signaling by CB2. While BCP did improve re-epithelialization, the
236 results of the cell migration studies showed that BCP's effect on re-epithelialization may be
237 more complicated than through the activation of CB2. Therefore, we examined whether
238 CB2 antagonists and agonists will affect re-epithelialization. AM630, an antagonist of CB2
239 [42] was daily injected 20 min before the daily application of BCP, CB2 agonist JWH133
240 [43] was topically applied instead of BCP to determine if it generates a similar impact as
241 BCP. Then tissues of the BCP group, the Oil group, the AMP630+BCP group, and the
242 JWH133 group were harvested on the 5th day post-surgery. Sections were stained with K14

243 antibody and the distance of migration from the edge of the wound was measured.
244 Consistent with our previous observations, topical application of BCP enhanced re-
245 epithelialization. CB2 agonist JWH133 significantly enhanced re-epithelialization compared
246 to the Oil group (Fig. 6). When CB2 antagonist AM630 was injected daily into mice treated
247 with BCP, the results were not clear. Re-epithelialization was not statistically different from
248 the Oil group but the variance was large and there was a trend towards differences
249 (P=0.071) (Fig. 6). These results suggest that there could be some other pathways involved
250 in the BCP enhanced re-epithelization of the wounds.
251
252 **Fig. 6. Re-epithelialization (K14+ distance from wound edge) in mice exposed to BCP,**
253 **Oil, CB2 agonist JWH133, and BCP+CB2 antagonist AM633**. **(a)** Length of K14+ staining
254 area from the boundary of the intact and wounded area to the center of the wound in skin
255 harvested on post-surgery day 5 from mice exposed to BCP, oil, JWH133 or injected CB2
256 antagonist AM630 daily before daily treatment with BCP. Dots indicate each data set and
257 the height of bars indicates the median. Horizontal lines indicate quartiles. ANOVA,
258 $F_{3,53}$=5.51, P=0.002) (ANOVA, $F_{3,53}$=5.51, P=0.002. Post-hoc pairwise analyses between BCP
259 vs. oil, Tukey's post-hoc pairwise comparison, P=0.002, CB2 agonist JMW133 group vs. oil
260 group, Tukey's post-hoc pairwise comparison, P=0.071, and CB2 antagonist AM630+BCP
261 group vs. BCP group, Tukey's pairwise comparison, P=0.097; BCP, n=9, Oil, n=10, JWH133,
262 n=8, AM630+BCP, n=7). **(b)** Representative images of JWH133 group and BCP+AM630
263 group. In: Intact area, W: wounded area. (147 words)
264

265 **BCP changes gene expression in the wounded skin**

266 In order to better predict the pathways through which BCP acts, we conducted RNA
267 sequencing and transcriptome analyses. The skin from mice 17 to 18 hours post-injury
268 treated with BCP or oil was used. The transcriptome of mice that were not injured (NT
269 group) was also analyzed to determine which gene expression changes are caused by
270 injury itself.
271 When a comparison was made between the BCP group vs. the NT group and the Oil
272 group vs. the NT group, the gene expression patterns of the BCP group and the Oil group
273 were similar (38 out of 50 top significant genes were common). This suggests that these
274 common genes could be genes that become modulated when there is skin injury (S5 Fig).
275 When comparison was made between the BCP group vs. the Oil group, significant
276 differences in gene expression between the BCP group and the Oil group were found (Fig
277 7). BCP-treatment significantly up-regulated a large number of genes, the 50 whose
278 expression changed the most are in Table 1. Twenty percent of the up-regulated genes
279 code for keratins (*Krt*) or keratin-associated proteins (*Krtap*) [44] (Table 1). Krtap genes
280 are expressed in cells of the hair shaft cortex [45], where we had observed an increased
281 number of BrdU+ cells (Fig. 3). Other than the possible role of BCP on enhancing re-
282 epithelialization, this result also suggests the possibility that exposure to BCP promotes
283 more complete skin regeneration and hair neogenesis. The remaining forty of the top 50
284 up-regulated genes code for functions in cell migration (e.g. *Adamts*) [46], cell fate
285 determination, and hair follicle formation (*Bambi, Msx2, Dlx3, Padi1, Hoxc13, S100a*) [47-
286 52]. These results overall suggest that BCP has impacts on hair follicle stem cell production
287 and skin regeneration to aid in wound healing.
288

289 **Fig 7. Results of RNA sequencing of post-surgery 17 hours skin and intact skin.**

290 Heatmap showing the top 50 significant gene expressions in the skin exposed to BCP (n=2)

291 or oil (n=3), 17 to 18 hours post-surgery (inflammation stage), and in the skin of mice

292 without skin excision (NT group) (n=3). Comparison between BCP vs. oil **(a)** showed a

293 clear difference between BCP and Oil. **(b)** Volcano plot from the comparison between BCP

294 vs. Oil. Y-axis shows log10 (p value) and X-axis shows log2 fold change value. (85 words)

295

Table 1 Top 50 genes altered in mice treated with oil and BCP. Top 50 genes were all up-regulated in the BCP group compared to the Oil group.

Genes	Log2FC	Pvalue	Family/roles and functions	References
Krtap3-1 *Krtap3-2* *Krtap3-3* *Krtap4-9* *Krtap16-1* *Krtap17-1*	8.355 3.195 5.357 8.410 9.052 5.949	1.43E-16 6.4E-19 3.6E-43 3.02E-13 8.86E-18 6E-25	Krtap family; keratin associated protein;	
Krt31 *K rt32* *Krt39* *Krt83*	9.963 2.876 4.537 8.568	9.34E-18 8.67E-17 2.64E-14 1.85E-14	Krt family; keratin	
Dok4	1.116	1.04E-16	Dok family; docking protein; "Associate with receptor tyrosine kinase c-Ret and function in c-Ret-mediated neurite outgrowth"; "play a positive role in activation of the MAP kinase pathway" (Grim et al. 2001)	Grim et al. 2001
Dlx3 *Dlx4os*	2.876 3.393	1.24E-20 1.99E-15	DLX family; distal-less homeobox; keratinocytes differentiation	Bhattacharya et al. 2017; Palazzo et al. 2017
Nkd2	1.739	5.68E-15	Naked cuticle family; a major component of Wnt signaling; "negatively regulates canonical Wnt signaling by binding Dishevelled" (Dsh) (Li et al. 2004)	Li et al. 2004
Ephb3	0.964	6.41E-15	Developmental process; embryogenesis	Flanagan and Vanderhaeghen 1998; Zhou 1998
Gabrp	2.536	5.91E-21		
Gpr37	2.350	4.81E-16		

Psors1c	3.526	3E-22	An immune system gene related to develop psoriasis, a disfiguring inflammatory skin disease	
Cpm	2.030	1.39E-13	Machrophage differentiation	
Pinlyp	3.894	1.67E-16		
Csdc2	3.974	8.42E-22	Hair follicle cycling	Yang et al. 2017
S100a7a	4.018	4.15E-21	"functions as a transglutaminase substrate/cornified envelope precursor, signal transduction protein, chemokine, and antibacterial protein in normal epidermis" (Eckert and Lee, 2006); Inflammation and cell migration; chemotaxis	Eckert and Lee 2006; Zwicker et al. 2012; Batycka-Baran et al. 2015
Unc5b	1.067	1.95E-17	Morphogenesis; Potential mediaters of beta-catenin signaing; angiogenesis	Lu et al. 2004; Zhang et al. 2008;
Adamts18	4.300	4.28E-14	Development, angiogenesis, coagulation	Wei et al. 2014; Kelwick et al 2015
Sptssb	4.234	8.74E-17	Axon	Zhao et al. 2015
Gm10318	10.288	1.12E-15	Nothing known so far	
Otop2	5.273	4.2E-19		
Tchhl1	10.815	1.37E-22	Expressed in basal layer of epidermis; expressed in the nuclei of cultured growing keratinocytes	Yamakoshi et al. 2013
Vsig8	7.709	2.77E-18	Hair shaft protein	Rice et al. 2011
Fam26d	10.723	2.77E-18		
Ly6g6d	6.345	5.34E-25		
Padi1	7.996	5.74E-14	Epidermal differentiation	Chavanas et al. 2006; Moelants et al. 2013
Bambi	3.486	1.67E-26	"Negatively regulates TGFbeta family signaling by a regulatory mechanism involving the interaction of signaling receptors with a pseudoreceptor" (Onichtchouk et al. 1999); mouse embryogenesis	Onichtchouk et al. 1999; Grotewold et al. 2001

Tchh	7.708	2.17E-16	Hair follicle inner root sheath	Yamamoto et al. 2009
Sytl2	1.916	3.27E-20	Cellular activity	Fukuda and Mikoshiba 2001; Li et al. 2018
Bean1	3.567	7.9E-15		
Zfp618	3.060	2.48E-14	Development; cerebellar neural stem/progenitor cells during development	Naruse et al. 2018
Msx2	3.792	6.03E-20	In epidermis, hair follicles and fibroblasts of developing fetal skin (Stelnicki et al 1997); in adult skin, confined to epithelial derived structures; hair cycle control and hair shaft differentiation (Kim and Yoon 2013)	Stelnicki et al. 1997; Kim and Yoon 2013)
Rtkn2	3.410	7.44E-14		
Lrrc75b	5.540	1.6E-18		
Hoxc13	2.829	2.56E-13		
Pm20d1	2.060	8.47E-15		
Rhpn2	1.681	3.56E-13		
D730001G18Rik	4.438	4.08E-48		
Foxn1	1.368	3.81E-15		
Car6	4.084	8.35E-33		
Slc40a1	1.727	8.58E-21		

Bhattacharya, S. J. et al. *Invest Dermatol*. **138**(5): 1052-1061 (2017).; Batycka-Baran, A. et al. *J Dermatol Sci*. **79**(3): 214-221 (2015).; Chavanas, S. et al. *J Dermatol Sci*. **44**(2): 63-72 (2006).; Eckert, R.L. & Lee, K.C. *J Invest Dermatol*. **126**(7): 1442-1444 (2006).; Flanagan, J.G., & Vanderhaeghen, P. *Annu Rev Neurosci*. **21**: 309-345 (1998).; Fukuda, M. & Mikoshiba, K. *Biochem Biophys Res Commun.* **281**(5): 1226-1233 (2001).; Grim, J. et al. *J Cell Biol*. **154**(2):345-354 (2001).; Grotewold, L. et al. *Mech Dev*. **100**(2): 327-330 (2001).; Kelwick, R. et al. *Genome*. **16**:113 (2015).; Kim, B.K. & Yoon, S.K. *J Dermatol Sci*. **71**(3): 203-209 (2013).; Li, C. et al. *PNAS* **101**(15): 5571-5576 (2004).; Li, X. et al. *Cell Tissue Bank*. **19**(3): 277-285 (2018).; Lu, X. et al. *Nature* **432**(7014): 179-186 (2004).; Moelants, E.A. et al. *Cytokines* **61**(1):161-167 (2013).; Naruse, M. et al. *Neurochem Res*. **43**(1): 205-211 (2018).; Onichtchouk, D. et al. *Nature* **401**(6752): 480-485 (1999).; Palazzo, E. et al. *Cell Death Differ*. **24**(4): 717-730 (2017).; Rice, R.H. et al. *J Invest Dermatol*. **131**(9): 1936-1938 (2011).; Stelnicki, E.J. et al. *Differentiation*. **62**(1): 33-41 (1997).; Wei, J. et al. *Front Biosci*. **19**:1456-1467 (2014).; Yamakoshi, T. et al. *Biochem Biophys Res Commun*. **432**(1): 66-72 (2013).; Yamamoto, S. et al. *Exp Dermatol*. **18**(2): 152-159 (2009).; Yang, M. et al. *Sci Rep*. **7**(1): 13502 (2017).; Zhang, Y. et al. *Development*. **135**(12).: 2161-2172 (2008).; Zhao, L. et al. *PNAS* **112**(42):12962-12967 (2015).; Zhou, R. *Pharmacol Ther*. **77**(3): 151-181 (1998).; Zwicker, S. et al. *Dtsch Med Wochenschr*. **137**(10): 491-494 (201

274 The transcriptome analysis prompted us to examine whether BCP treatment affected
275 genes known as hair follicle stem cell markers [38]. The hair follicle bulge markers *Gli1*,
276 *Lgr5*, and *Sox9* were significantly up-regulated (Log2FC, 2.4605, 1.236, 0.5377,
277 respectively) in the BCP group compared to the Oil group (see bottom table in Fig. 8). Hair
278 follicle infundibulum marker *Lrig1* was also significantly up-regulated by 40% (Fig. 8,
279 log2FC 0.4035). These results on up-regulation of hair follicle bulge markers suggest that
280 BCP treatment can stimulate hair follicle stem cell production.
281
282 **Fig 8. Comparison of the expression of hair follicle marker genes**. Hair follicle genes
283 related to the bulge were significantly up-regulated in the mice exposed to BCP compared
284 to the Oil group. P-Values show the results of comparison between the BCP and the Oil
285 groups. *: P<0.05, **: P<0.01, ***: P<0.001. (50 words)
286
287 The inflammation stage of wound healing starts immediately after injury and pro-
288 inflammatory cytokine levels usually peak within the first 10 to 20 hours [53,54], then
289 decrease for 2 days. The main source of cytokines is known to be neutrophils [53]. In our
290 study, we used 17 to 18 hours post-injury skin and, of the pro-inflammatory cytokines, IL-
291 1β and IL6 genes were significantly down-regulated in the BCP group compared to the Oil
292 group (Table 2). This suggests that BCP treatment suppressed acute inflammation after
293 skin exicision (Table 2). Studies have shown that there is a rebound in the inflammatory
294 cytokines after 3 days, when fibroblasts migrate and new granulation tissues are formed,
295 which suggest that the cytokines during the 'rebound' stage may play a role in wound
296 *remodeling* [53]. Using the tissue harvested on post-surgery day 4, we examined the

297 expression of the pro-inflammatory cytokines IL-1β and TNFα (Fig. 9a and b). IL-1β
298 expression was especially strong in the wound bed of the BCP-treated mice. IL-1β and
299 TNFα were expressed 2.7 times higher and 2.0 times higher, respectively, at the wound bed
300 in the BCP group when compared to the Oil group (compared using color intensity in the
301 image field). Apoptosis is involved in various stages of tissue repair with its main role in
302 eliminating unwanted cells. If the acute inflammation immediately after injury is
303 suppressed, it is possible to expect that the apoptosis rate might be suppressed in the BCP
304 group. We conducted a terminal deoxynucleotidyl transferase (TdT) dUTP nick-end
305 labeling (TUNEL) assay to detect apoptotic cells. TUNEL+ cells were abundant in the wound
306 bed of both BCP-treated and oil-treated wounds when compared to the intact area.
307 However, TUNEL staining was much stronger in the Oil-treated group (2.0 times higher in
308 color intensity in the Oil group compared to the BCP group). In the BCP-treated wounds,
309 TUNEL+ cells were present in the bottom of the epidermis and dermis close to the wound
310 edge (Fig. 9c). These results suggest that, in the BCP group, pro-inflammatory cytokines
311 are suppressed immediately following injury which may have produced reduced apoptosis
312 at 4 days post-injury. Although the expression of pro-inflammatory cytokines is suppressed
313 in the BCP group during the early stage after injury, they become more expressed than the
314 Oil group at post-surgery day 4, which is when they are at the cell proliferation stage.
315 Further studies are required to precisely determine the roles of these cytokines in the
316 differences observed in wound healing between the BCP and Oil treated wounds.
317
318 **Table 2. Expression of pro-inflammatory cytokines in the BCP group compared to the**
319 **Oil group.**

Gene	Log2FC	Pvalue
IL-1b	-1.236	0.003
IL6	-1.100	0.002
Tnf	-0.571	0.052
Mmp8	-2.06	9.00E-04
Mmp10	-0.667	0.033
Mmp16	-0.948	0.012
Mmp19	-1.069	0.012
Mmp28	-0.72	0.003
Casp4	-0.691	1.10E-03
Casp8	-0.508	5.17E-06
Casp14	0.76	0.001

Fig. 9. IL-1β, TNFα in the skin at the wound bed and close to the wound, and TUNEL staining of the skin at the wound bed and close to the wound. **(a)** IL-1β (red and purple) expression in the BCP and the Oil group. Blue color as well as purple color is Draq 5+ cells. Green is autofluorescence. **(b)** TNFα expression (red and purple) expression in the BCP and Oil group. Blue color as well as purple color is Draq 5+ cells. Green is autofluorescence. **(c)** TUNEL staining with double staining with Draq 5. Green and light blue is TUNEL+ cells. Blue and light blue is Draq5+ cells. Scale bars are μm. (110 words)

CB1 gene expression was not significantly different between the BCP and the Oil group, whereas CB2 gene was, to our surprise, down-regulated in the BCP group in the 17~18 hours post-injury skin. Recent studies have shown that Transient Receptor Potential (TRP) channels become activated by some phytochemicals [55]. We examined the expression of genes related to TRP channels and found that TRPM1, TRPM6, TRPV4, and TRPV6 were significantly up-regulated and TRPM2 and TRPM3 were significantly down-regulated in the BCP group compared to the Oil group (Table 3). Importantly, there are growing number of

336 papers showing the roles of TRP channels in the initiation of pain and itch perception as
337 well as epidermal homeostasis and hair follicle regulation, suggesting that the TRP
338 channels function as 'ionotropic cannabinoid receptors' [56]. Of the TRP channels
339 designated as putative ionotropic cannabinoid receptors [56], the one that overlaps with
340 TRP channels showing significant change after exposure to BCP was TRPV4, which showed
341 significant up-regulation. TRPV4 is expressed in various cell types including sensory
342 neurons and is considered to be a mechano/osmosensitive channel [57]. The results of our
343 study and recent studies on the roles of TRP channels suggest that TRP channels could be
344 involved in enhanced re-epithelialization by BCP.
345
346 **Table 3. Expression of cannabinoid receptors and TRP channel genes.** Genes up-
347 regulated in the BCP group compared to the Oil group are written in red color and down-
348 regulated genes are written in blue color. Genes written in black are not significantly
349 different between the BCP and the Oil group. Genes written in bold type have P values over
350 E-5. NA in P-Value is an outlier compared to other genes presumably because of its
351 extremely high expression in the BCP group compared to the Oil group.

Gene	Log2FC	Pvalue	
CB1 (cnr1)	-0.463	0.641	
CB2 (cnr2)	-0.755	0.028	pain, inflammation
TRPA	not found		
TRPC1	0.023	0.932	
TRPC2	0.350	0.326	
TRPC3	-0.047	0.937	
TRPC4	-0.083	0.861	
TRPC6	-0.157	0.824	
TRPM1	4.156	NA	melanin synthesis
TRPM2	-1.530	0.006	cutaneous pain sensation
TRPM3	-0.902	0.047	
TRPM4	0.130	0.370	

TRPM6	0.604	0.004	magnesium transport
TRPM7	-0.041	0.818	
TRPM8	2.582	0.427	
TRPV1	-0.236	0.635	
TRPV2	-0.391	0.125	
TRPV3	0.171	0.452	
TRPV4	0.586	0.008	interacts with beta-catenin
TRPV6	1.527	3.00E-10	calcium absorption calcium dependent cell proliferation inhibition of apoptosis

352

353

354 Ingenuity pathway analysis® (IPA®) was performed using the gene expression results.
355 In the comparison of the BCP vs. Oil group, signaling pathways related to inflammation and
356 the immune system (TREM1 signaling) [58]were suppressed in the BCP group (S6 Fig.). In
357 addition, genes that encode functions for cell proliferation and migration (e.g. the sonic
358 hedgehog pathway, the planar cell polarity, the signaling pathway, fibroblast growth factor
359 signaling pathway, and Wnt beta-catenin signaling pathway [S7 Fig. a, b, c, d]) were
360 activated compared to the Oil group. Table 4 summarizes the genes in these signaling
361 pathways that became significantly up/down-regulated in the BCP group compared to the
362 Oil group. In each of these pathways, there were genes whose expression was dramatically
363 increased (bold in Table 4). These could be the core genes affected by BCP: hedgehog
364 interacting protein gene (*hhip*), sonic hedgehog gene (*shh*), and dual specificity protein
365 phosphatase CDC14a (*cdc14a*) in the sonic hedgehog signaling pathway [59], frizzled-5
366 (*fzd5*), wingless-type MMTV integration site family member 5a, 10b, 11 (*wnt5a, 10b, 11*) in
367 the planar cell polarity signaling pathway [60], fibroblast growth factor 22 and 23 (*fgf22,*
368 *fgf23*) and phosphoinositide-3-kinase regulatory subunit 3 (*pik3r3*) in the fibroblast

369 growth factor signaling pathway [61], and *wnt5a, 10b, 11*, whitefly-induced tomato gene
370 (*wfi1*), transcription factor sox4 (*sox4*), and lymphoid enhancer-binding factor 1 (*lef1*) in
371 the Wnt/beta-catenin signaling pathway [62]. Studies have found that, in the case of adult
372 skin, hedgehog signaling is involved in epidermal homeostasis, *i.e.*, the hair cycle and
373 regrowth of hair [63]. *GLI1* is expressed in the hair follicle bulge and, when sonic hedgehog
374 secreted from sensory neurons surrounding the hair follicle bulge stimulates the Gli1+ cells
375 in the upper region of the bulge, the Gli1+ cells convert to multipotent stem cells. These
376 multipotent stem cells migrate to epidermis and contribute to wound healing by becoming
377 epidermal stem cells [64]. The planar cell polarity pathway is known to be involved in
378 collective and directed cell movements during skin wound repair [65-68] and coordinating
379 the directions of cell migration [67]. Studies using transgenic mice have shown that the
380 role of fibroblast growth factor signaling includes keratinocyte proliferation [68]. Overall,
381 the results on gene expression in our study suggest that exposure to BCP activated the
382 pathways in a way to enhance 1) conversion of hair follicle bulge stem cells to epidermal
383 stem cells, 2) keratinocyte cell proliferation, 3) coordinated and directed cell movement,
384 which may have contributed to enhanced re-epithelialization by exposure to BCP.
385
386 **Table 4. Significantly up/down-regulated genes in *shh, pcp, fgf, and wnt/beta-***
387 ***catenin* signaling pathways after exposure to BCP.** Genes with log fold change over 1 are
388 shown. Up-regulated genes are written in red, and down-regulated genes are written in
389 blue. Results of genes with over E-05 P-values are shown in bold letters. NA in P-Values is
390 an outlier compared to other genes presumably because of its extremely high expression in
391 the BCP group compared to the Oil group.

Pathway	*Gene*	Log2FC	PValue
sonic hedgehog	*Hhip*	3.202	3.44E-06
	Ptch1	1.564	1.02E-04
	Ptch2	3.374	2.02E-04
	Shh	5.995	NA
	Gli1	2.46	1.76E-05
	Gli2	1.179	1.00E-03
planar cell polarity	*Fzd5*	1.086	7.48E-08
	Ror2	1.627	5.40E-05
	Wnt5a	1.606	7.84E-10
	Wnt10b	1.613	1.58E-08
	Wnt11	1.997	6.53E-11
	Ndp	1.2746	1.84E-02
fibroblast growth factor	*Fgf5*	2.109	2.40E-05
	Fgf22	1.292	1.49E-08
	Fgf23	-1.809	1.97E-11
	Tlr9	-1.953	3.60E-04
	Pik3R3	1.081	1.77E-06
Wnt beta-catenin	*Wnt5a*	1.606	7.84E-10
	Wnt10b	1.613	1.58E-08
	Wnt11	1.997	6.53E-11
	Wfi1	1.778	4.18E-09
	Sox4	1.662	1.12E-10
	Sox5	1.821	4.81E-05
	Sox13	1.406	9.10E-04
	Lef1	3.152	2.48E-10

Sex differences in the impact of BCP

These results summarized above are based on experiments using female mice. Previous studies have shown sex differences in the morphology and physiology of mouse skin, with female mice having a 40 % thicker epidermis than males [69]. In addition, androgen receptors have an inhibitory influence on wound healing in males [70], which may hinder the impact of BCP.

400 We tested whether the influences of BCP on wound healing in male mice is similar to its
401 influences in females and found no statistically significant differences in re-epithelialization
402 between the BCP and Oil groups in males (based on K14 staining) (Fig 10). Whether males
403 need a higher concentration of BCP to induce its impact or whether BCP does not affect
404 males at all needs to be addressed in future.
405 Sex steroids are known to affect wound healing [71], androgen receptors inhibit wound
406 healing [60] whereas estrogen receptors accelerate it [32]. The re-epithelialization in the
407 Oil control group for males was similar to that of the Oil group of female mice (Fig 10),
408 which suggests that sex hormones did not suppress re-epithelialization in males.
409
410 **Fig 10. Influence of BCP on re-epithelialization in male and female mice.** Length of
411 K14+ staining area from the boundary of the intact and wounded area to the center of the
412 wound in skin harvested on post-surgery day 4 from mice exposed to BCP or oil. Bar
413 indicates median and line indicates 25 and 75% quartile. ANOVA, BCP vs. oil, $F_{1,66}$=14.793,
414 P<0.001; gender, $F_{1,66}$=30.761, Tukey's post-hoc test, ***: P<0.001; females, BCP, n=16, oil,
415 n=16, males, BCP, n=23, oil, n=15 (76 words)
416

417 Olfactory receptors are not involved in wound healing

418 BCP is an odorant. When mice are topically treated with BCP, they are exposed to its
419 smell and there is a possibility that the olfactory system has some role in the BCP mediated
420 enhanced re-epithelialization. In addition, olfactory receptors are expressed in non-
421 olfactory tissues. A synthetic analogue of sandalwood odorant, sandalore, is the ligand of
422 the olfactory receptor gene OR2AT4 and that OR2AT4 receptors are expressed in human

423 skin [72]. Thus odorants can directly produce an impact on non-olfactory tissues like skin
424 tissues [72] other than through the route of the olfactory system to the brain, affecting
425 emotional status [73]. There is a possibility that the impact of BCP was mediated by
426 olfactory receptors expressed in the skin.

427 To examine if the olfactory system and/or olfactory receptors expressed in the skin has
428 some role in enhanced re-epithelialization by exposure to BCP, we conducted multiple
429 experiments. First we tested if mice can smell BCP by testing the expression of an
430 immediate early gene protein in the olfactory bulb of mice exposed to BCP and found clear
431 expression of c-FOS protein, suggesting that it is highly likely that mice can smell BCP (S8
432 Fig.). Then we tested whether exposure of injured mice to BCP only through the air would
433 produce a similar impact as topical application, and found no improved re-epithelialization
434 (S9 Fig). It was clear that the olfactory system was not significantly involved in the impact
435 of BCP on re-epithelialization.

436 To examine if olfactory receptors expressed in the non-olfactory system are involved,
437 we first examined the olfactory epithelium after exposure of non-injured mice to BCP for
438 one hour to identify the olfactory receptor genes for BCP using pS6-IP RNAseq [74]. We
439 could narrow down the candidates of olfactory receptor genes for BCP (S2 Table). It is
440 known that odorants stimulate a limited number of types of olfactory receptors [75, 76]. As
441 the BCP we used was not 100 % in purity, multiple olfactory receptor genes were up-
442 regulated following exposure to BCP with *Olfr340* showing the largest fold change and
443 significant P-Value (S2 Table). After this step, we analyzed the results of RNA sequencing of
444 the skin to determine if the olfactory receptor genes up-regulated in olfactory epithelium
445 by exposure to BCP are expressed in skin and are up-regulated after topical application of

446 BCP. There were many olfactory receptor genes expressed in the skin (S3 Table), and one
447 of them overlapped with the olfactory receptor genes up-regulated in olfactory epithelium
448 (*Olfr111*), but none of them were up-regulated specifically in the BCP group. From these
449 results, we conclude that olfactory receptors expressed in skin are not involved in the
450 enhanced re-epithelialization by exposure to BCP.
451

452 Synergetic influences by exposure to BCP

453 Wound healing starts from the inflammatory stage and shifts to the cell proliferation
454 stage. Since BCP is an agonist of CB2, we had assumed that it can improve wound healing
455 by decreasing pain and reducing pro-inflammatory signals and speed up the shift to the cell
456 proliferation stage. However, our results suggests that BCP may directly impact cell
457 proliferation and cell migration concomittent with reduced inflammation. BCP also
458 stimulates mitogenesis of hair follicle stem cells. Hair follicle stem cells participate in re-
459 epithelialization when there is a cutaneous wound [41, 51], our study suggests that
460 enhanced re-epithelialization by exposure to BCP is mediated by BCP stimulated
461 production of hair follicle stem cells in the bulge, and their migration to epidermis and to
462 wound bed.
463 BCP is known to suppress apoptosis [77] and necroptosis [78], raising the possibility
464 that suppression of cell death enabled higher cells survival and proliferation. The
465 suppression of *Septin4* (*Sept4*) has been shown to protect cells from cell death and promote
466 wound healing [79], however, *Sept4* was not up-regulated in our study and seemed to be
467 not involved in BCP enhanced re-epithelialization. It is possible that exposure to BCP

468 generates a specific wound healing environment by up-regulating the genes related to
469 embryonic growth as was suggested from our results on transcriptome analyses.
470 Our study focused on the early stage following skin excision. Studies have shown that
471 oxidants from inflammatory cells are involved in fibrotic healing (scarring) [80, 81], which
472 suggests that suppression of inflammation through activation of CB2 by BCP, in addition to
473 up-regulation of genes related to embryonic growth would have a high possibility of
474 reducing scar formation. These possibilities need to be addressed in future by testing the
475 influence of exposure to BCP on the late stage after injury.
476

477 ## Odors affect us more than we think

478 It has been several decades since the first report that olfactory receptors are expressed
479 in non-olfactory regions [82] and that odors have functions other than olfactory and
480 pheromonal communication [83]. Our observations that BCP activates multiple types of
481 receptors in the skin further unveils the complexity of chemical signaling. Although we
482 humans typically rely on visual and auditory stimuli in communication, it is important to
483 understand how odors in the environment, whether it is from other individuals [1] or from
484 plants [2-6], could be affecting our condition. In addition, BCP is but one component
485 commonly found in essential oils of herbal extracts. Further examination of the
486 compounds in herbal extracts could lead to additional useful molecules that could benefit
487 our health.
488

489 # Materials and methods

490 ## Mice strains

491 We used a standard murine model for wound healing. Mice were used between 8 to 10
492 weeks in age in *in vivo* experiments. C57BL/6J, and CB2-/- mice were used in experiments.
493 Primary cells for *in vitro* experiments were obtained from P0 to P1 neonate pups or adult
494 mice from C57BL/6J, or CB2-/- mice. In *in vivo* experiments, C57BL/6J mice were used. All
495 mice were kept on a 14:10, L/D light cycle, and water and food were provided *ad libitum*.
496 All the procedures were following a protocol (#16-022) approved by the Indiana
497 University Institutional Animal Care and Use Committee (IACUC).
498

499 ## Surgery

500 We studied small full-thickness excisions on the backs of adult mice and developed
501 methods to hold the treatment buffer solution on the wounded area (S1 Fig a). Hair of the
502 dorsal area was removed and the area for surgery was cleansed using betadine and 70%
503 ethanol. A small piece of the dorsal skin of a mouse was excised (< 5mm x 5mm) under
504 anesthesia. A silicone ring was attached to the wounded area using a liquid sealing
505 bandage (S1 Fig a center) (OD: 15mm, ID: 8mm, thickness, 3mm). This ring served as a
506 reservoir and 50 μL of BCP (50 mg/kgbw; 0.2nM) (W225207, Sigma-Aldrich, Co. St. Louis,
507 MO) diluted in olive oil, or olive oil as control (O1514, Sigma-Aldrich, Co. St. Louis, MO),
508 was placed in the reservoir. The gas chromatography-mass spectrometry (GC/MS) analysis
509 of the BCP standard showed that it contained 81.8% BCP and 14.0% α-caryophyllene (α-
510 humulene). The remaining 4.2% consisted of 1.6% caryophyllene oxide and minor amounts
511 of other molecular weight 204 sesquiterpenes (0.1-0.8% each) (S4 Fig., S1 Table).

512 Molecular weights were calculated by the amount of BCP (81.9% of the volume converted
513 to molecular weight).
514 The ring was covered with a baked PDMS lid (polydimethylsiloxane) (Dow Corning
515 Sylgard® 184 Silicone Elastomer Kit; Dow Corning, Auburn MI) and sealed with liquid
516 bandage to hold the BCP media or olive oil. A gauze bandage was used to loosely cover the
517 body to prevent the mouse from removing the ring with PDMS lid (S1 Fig 1a, right down).
518 The bandage and buffer media were removed daily and replaced with a new bandage and
519 buffer media. The wounded area was collected on the 3rd, 4th, and 5th day, and immediately
520 fixed with 10% formalin for one day, then soaked in 70% ethanol.
521

522 Gas chromatography – mass spectrometry (GC/MS) analysis of
523 BCP

524 BCP was diluted to 180 ng/μL with a tert-butyl methyl ether solvent (99+%, Aldrich
525 Chemical Company, Milwaukee, WI). The BCP composition was analyzed using 2 μL of the
526 diluted BCP in a thermal desorption tube of the Thermal Desorption Autosampler and
527 Cooled Injection System (TDSA-CIS 4 from Gerstel GmbH, Mülheim an der Ruhr, Germany)
528 connected to an Agilent6890N Gas chromatograph – 5973iMSD Mass spectrometer (Agilent
529 Technologies, Inc., Wilmington, DE). BCP components were identified with spectra through
530 the NIST Mass Spectral Search Program for the NIST/EPA/NIH Mass Spectral Library
531 (Version 2.0 a, 2002). Additionally, the mass spectra and Kovats retention index matches
532 were verified with the reference spectra from Adam (2001) [84]. Caryophyllene oxide was
533 verified with the standard (99%) from Sigma-Aldrich (St. Louis, MO).
534

535 ## CB2 agonist and antagonist treatment

536 CB2 agonist JWH133 (1 μM; Cat. 10005428, Cayman Chemical Co., Ann Arbor, MI),
537 dissolved in alcohol and kept at -20°C, was dissolved in olive oil after the alcohol was
538 evaporated and used instead of BCP in the daily treatment on the wounded area. CB2
539 antagonist, AM630 (4 mg/kgbw (7.9 μM/kgbw); SML0327, Sigma-Aldrich Corp. St. Louis,
540 MO) was dissolved in saline and injected 20 min before the daily treatment of BCP.
541

542 ## Immunofluorescence staining to evaluate re-epithelialization

543 Mice were euthanized by cervical dislocation and the wounded areas were harvested,
544 fixed in 10% formalin at room temperature and then in 70% ethanol at 4°C until they were
545 embedded in paraffin. Samples were sectioned at 10 μm, deparaffinized and hydrated,
546 went through antigen retrieval using the sodium citrate buffer (10mM, >95°C for 20 to 30
547 min), blocked with 10% NGS, and primary stained (see below for antibodies) overnight at
548 4°C. Then sections were washed, secondary stained, nuclear stained using Draq 5, washed
549 (3 times), and covered with Prolong Diamond (ProLong™ Diamond Antifade Mountant
550 P36965, Thermo Fisher Scientific).
551 Antibodies used are as follows: proliferating cell nuclear antigen (PCNA (PC10) mouse
552 mAb #2586, Cell Signaling Technology, Danvers, MA, 1:1000), keratin 14 (K14, rabbit pAb,
553 905301, 1:1000, BioLegend, San Diego, CA), PDGFRalpha (mouse mAb, sc-398206, Santa
554 Cruz Biotechnology, CA, 1:1000), vimentin (rabbit, 10366-1-AP, Protein Tech, 1:500),
555 estrogen receptor alpha (Eralpha, mouse mAb, sc-51857, sc-8002, Santa Cruz
556 Biotechnology, 1:250), filaggrin (rabbit pAb, BioLegend, San Diego, CA, 1:1000), TNFalpha
557 (rabbit pAb, ab6671, Abcam, 1:100), IL-1beta (rabbit pAb, ab9722, Abcam, 1:100). Alexa

558 fluor 594 anti-rabbit and Alexa fluor 488 anti-mouse (both Invitrogen, 1:500). Stained
559 sections were observed using laser scanning confocal microscope Leica SP5 at the IUB
560 Light Microscope Imaging Center.
561

562 TUNEL staining

563 Mice were euthanized by cervical dislocation and the wounded area was harvested,
564 fixed in 10% formalin at room temperature and then in 70% ethanol at 4°C until embedded
565 in paraffin. Samples were sectioned at 10 μm, deparaffinized and hydrated. TUNEL staining
566 was conducted following manufacturer's protocol (In Situ Cell Death Detection Kit, Version
567 17, Roche Diagnistics GmbH, Mannheim, Germany). Briefly, slide glasses were first rinsed
568 with PBS for 5 min twice, then went through antigen retrieval using sodium citrate buffer
569 (10mM, >95°C for 20 to 30 min), and rinsed with PBS for 10 min three times. Blocked with
570 0.1 M Tris-HCl, pH7.5 with 3% BSA and 20% normal bovine serum for 30 min. Slides were
571 rinsed twice with PBS for 10 min twice. Then TUNEL reaction mixture were added and
572 slides were incubated for 1 hour at 37°C. Slides were rinsed for 10 min once, stained with
573 Draq5 for 10 min at room temperature, and rinsed for 10 min three times. Finally, slides
574 were covered with Prolong Diamond (ProLong™ Diamond Antifade Mountant P36965,
575 Thermo Fisher Scientific). Stained sections were observed using laser scanning confocal
576 microscope Leica SP5 at the IUB Light Microscope Imaging Center.
577

578 BrdU injection and staining

579 On post-surgery day 4, mice were injected with bromodeoxyuridine (BrdU) (300
580 mg/kgbw) twice every 2 hours, and the skins were harvested 2 hours after the second

581 injection. Harvested skin was fixed with 10% formalin, and then with 70% ethanol on the
582 following day. Samples were embedded in paraffin and cut into sections using microtome
583 at 10 μm. Sections were then deparaffinized and hydrated, went through antigen retrieval
584 using 4N HCl at 37°C for 30 min, washed with 0.1M PBS, blocked with 10% NGS, and went
585 through overnight staining at 4°C with anti-BrdU (1:300, rat, Accurate Chemical Co.
586 #OBT0030). On the second day, sections were washed with 0.1M PBS, stained with anti-rat
587 Alexa fluor 488 (1:500, Invitrogen) at room temperature, washed, stained with Draq5,
588 washed, and covered after placing one drop of Prolong Diamond (ProLong™ Diamond
589 Antifade Mountant P36965, Thermo Fisher Scientific). Sections were observed using laser
590 scanning confocal microscope (Leica DMI 6000 CS inverted microscope) in the IUB Light
591 Microscope Imaging Center and analyzed using Fiji/ImageJ software.
592

593 Immediate Early Gene (*c-fos*) protein expression experiment and
594 staining

595

596 Each mouse was exposed to BCP or male murine pheromone 2-sec-butyl-4,5-
597 dihydrothiazole (SBT) (250ppm, positive control) [85, 86] for 1 hour in a clean cage. Then
598 mice were anesthetized with 2.5% isoflurane and cardiac perfused with saline for 2 min,
599 followed by 4% paraformaldehyde for 6 to 7 min. The brains were dissected out and post-
600 fixed with 4% paraformaldehyde overnight at 4°C, transferred to PBS with 15% sucrose
601 and kept at 4°C. The brains were embedded in OCT on dry ice and cryosectioned using
602 Leica CM1850 at 20 μm and kept at -20°C until use.

603 For the staining of c-*fos* gene protein, the brain sections were washed 3 times for 10
604 mins with 0.1M PBS, blocked with 10% NGS, 0.5% Triton X-100 in 0.1M PBS for 1 to 2
605 hours, and went through primary staining with anti-cFOS (Invitrogen OSR00004w, rabbit,
606 1:250; Abcam ab190289, rabbit, 1:2000) overnight at 4°C. Then sections were washed 3
607 times for 10 mins and went through secondary staining (Alexafluor 594, anti-rabbit,
608 1:500), washed with 0.1M PBS, stained with Draq5, washed (0.1M PBS 3 times each 10
609 mins), and covered with Prolong Diamond. Bregma distance about 4.28mm was used in the
610 comparison. The stained sections were imaged using laser scanning confocal microscope
611 Leica SP5 at the IUB Light Microscope Imaging Center. The numbers of cfos+ cells in the
612 whole glomerular layer, external plexiform layer, mitral layer, internal plexiform layer, and
613 granule cell layer of olfactory bulbs were counted using Fiji/Image J.
614

615 **Isolation of primary cells**

616 Fibroblast isolation: Mice (neonate or adult) were euthanized by cervical dislocation and
617 cleansed using betadine, sterlized water, and 70% ethanol. The harvested skins were
618 treated with 0.25% trypsin (Gibco, 15050065, Waltham MA) at 4°C overnight. Dermis was
619 collected after trypsin treatment, minced and pipetted to dissociate, and incubated at 37°C
620 with collagenase A buffer in cell culture media (1 mg/mL). Following the incubation, the
621 buffer with dissociated cells was filtered using 100 μL strainer, and centrifuged at 500 X G
622 for 8 min. Supernatant was removed and the pellet was re-suspended in CnT-PR-F media
623 (CELLnTECH; Zen-Bio, Research Triangle Park, NC), filtered with 40 μm strainer, and
624 centrifuged again at 500 X G for 8 min. Following another re-suspension to new culture
625 media, cells were seeded on petri dishes to culture at 37°C with 5% CO_2.

626 Keratinocytes: Skins were collected from neonate mice after the mice were decapitated and
627 cleansed. Collected skins were placed in petri dish with 0.25% Trypsin (Gibco, 15050065,
628 Waltham MA), with their epidermis side up and above the Trypsin buffer, at 4°C for 6 to 8
629 hours. Then the epidermis of the skin was removed from dermis, minced and pipetted to
630 dissociate in the trypsin buffer, filtered using 70 or 100 μm strainers, and centrifuged at
631 500 X G or 800G for 8 min. Supernatant was removed and the pellet was re-suspended in
632 high calcium DMEM medium ((Gibco, 10569-010, Waltham MA) supplemented with FBS
633 (10%), p/s, and Glutamax), filtered using 40 μm, centrifuged again and resuspended with
634 the high calcium DMEM medium. Then cells were seeded on Collagenase I coated petri
635 dishes (Collagen I, Coated Plate 6 Well, Gibco Life technologies A11428-01, Waltham MA),
636 incubated at 32 to 35°C[45] with 5% CO_2 with high calcium DMEM medium overnight[46]. On
637 the following day, culture medium was replaced with low calcium medium (CnT-PR,
638 CELLnTECH; Zen-Bio, Research Triangle Park, NC) and penicillin streptomycin (1140122,
639 ThermoFisher Scientific, Waltham MA).
640

641 ## Chemotaxis assay and scratch tests

642 Chemotaxis assay: Primary cultured cells (300 μL) were seeded in the inserts of 24 well cell
643 migration plate (Cell Biolabs Inc, CBA100, CytoSelect 24 well cell migration assay kit) with
644 500 μL of DMEM cell culture media containing BCP (5 μL in 10 μL of DMSO in 10mL of cell
645 culture media) or DMSO (control; 10 μL of DMSO in 10 mL of cell culture media) in the well,
646 and incubated at 37°C and 5% CO_2 for 1 day (approximately 18 to 24 hours). Then the
647 inserts were washed with water and observed under microscope, photographed using

648 EVOS XL Core (ThermoFisher Scientific, Waltham MA), and the number of the cells on the
649 outside bottom of the insert was counted using Fiji/ImageJ.
650 Scratch tests: Primary cultured cells were seeded in 12 well plates. Two days later the
651 culture media was changed to either 2 mL of DMEM cell culture media containing BCP (0.06
652 μL in 10 μL of DMSO in 10 mL of cell culture media) or DMSO (control; 10 μL of DMSO in 10
653 mL of cell culture media) and the surface of the bottom of the wells was scratched with the
654 tip of 1mL pipet tips. Photos were taken immediately after the scratches were made, 6
655 hours later, and 1 day later. Widths of the scratch line were measured using Fiji/Image J.
656

657 **Time lapse *in vitro* observation of cell proliferation**

658 Primary cultured cells were exposed to BCP in DMEM culture media or DMSO (control)
659 in DMEM culture media on the next day after the cells were seeded on petri dishes with
660 cover glass bottom (12-567-401, Thermo Scientific™ Nunc™). Immediately after the
661 media was changed to the media with BCP or the media with DMSO alone, cells were
662 cultured on an Olympus OSR Spinning Disk Confocal microscope with Tokai Hit Stage Top
663 Incubation system kept at 37°C and 5% CO_2. DIC images were taken every 3 mins for 7
664 hours using a Hammamatsu Flash 4V2 camera and movies were generated using
665 Metamorph software. Obtained images were played and the number of dividing cells were
666 counted.
667

668 **Transcriptome analyses using skin**

669 The wounded part of the skin was exposed to either BCP or olive oil (control) and the
670 tissues were harvested 17 hours later. This was based on the study which reported the

671 time course in the expression of genes related to inflammatory responses showing the peak
672 within the first 20 hours [54]. Tissues from another group of mice were harvested similarly
673 but without wound (no-injury control). The wounded area and its surrounding area (2 x 2
674 cm) were immediately dissected out and RNA extraction was conducted using Maxwell®
675 RSC simplyRNA Tissue Kit (AS1340, Promega, Madison WI) following the manufacturer's
676 protocol. The volume of extracted RNA was measured using Epoch™ Microplate
677 Spectrophotometer (BioTek, Winooski, VT) with Take 3 Micro-Volume Plates (BioTek,
678 Winooski, VT) and Gen5 Microplate Reader and Imager Software (BioTek, Winooski, VT).
679 The integrity was analyzed with Agilent Technologies 2200 Tape Station (Agilent
680 Technologies). The input was quantified by using Qubit RNA BR Assay Kit and RNA-seq was
681 conducted using NextSeq Series RNA-seq Solution (Illumina) at the Center of Genomics and
682 Bioinformatics, IUB. Samples were prepared using TruSeq Stranded mRNA HT Sample
683 Prep Kit (Illumina). Sequencing was performed using an Illumina NextSeq 500/550 Kits v2
684 reagents with 75 bp sequencing module generating 43 bp paired-end reads. After the
685 sequencing run, demultiplexing was performed with bcl2fastq v2.20.0.422.
686

687 pS6-IP RNA-Seq analyses using olfactory epithelium

688 To perform pS6-IP RNA-Seq, we used 4 pairs of litter-matched mice. We used both male
689 and female mice in both control and experimental conditions with no specific orientation.
690 Single pairs of mice were habituated in clean paper tubs in a fume hood for 1 hour.
691 Following habituation, mice were transferred to another paper tub with an uni-cassette
692 containing a 2 cm x 2 cm filter paper spotted with either water (control) or 1% (v/v) 10 L
693 BCP dissolved in water (experimental) for 1 hour.

694 Following odor stimulation, mice were killed and the olfactory epithelium (OE) was
695 dissected in 25 mL of dissection buffer (1× HBSS [Gibco, with Ca^{2+} and Mg^{2+}], 2.5 mM
696 HEPES [pH 7.4], 35 mM glucose, 100 μg/mL cycloheximide, 5 mM sodium fluoride, 1 mM
697 sodium orthovanadate, 1 mM sodium pyrophosphate, 1 mM beta-glycerophosphate) on
698 ice.
699 The dissected OE was transferred to 1.35 mL of homogenization buffer (150 mM KCl, 5
700 mM $MgCl_2$, 10 mM HEPES [pH 7.4], 100 nM Calyculin A, 2 mM DTT, 100 U/mL RNasin
701 (Promega), 100 μg/mL cycloheximide, 5 mM sodium fluoride, 1 mM sodium orthovanadate,
702 1 mM sodium pyrophosphate, 1 mM beta-glycerophosphate, protease inhibitor (Roche, 1
703 tablet per 10 ml)) and homogenized three times at 250 rpm and nine times at 750 rpm
704 (Glas-Col). The homogenate was transferred to a 1.5 mL lobind tube (Eppendorf), and
705 centrifuged at 2,000 X G for 10 min at 4°C. The supernatant was then transferred to a new
706 1.5 mL lobind tube, to which 90 μL 10% NP-40 (vol/vol) and 70 μL 300 mM DHPC (Avanti
707 Polar Lipids) were added. The mixture was centrifuged at 17,000 X G for 10 min at 4°C.
708 The supernatant was transferred to a new 1.5 mL lobind tube and mixed with 6 μL pS6
709 antibody (Cell Signaling, D68F8). Antibody binding was allowed by incubating the mixture
710 for 1.5 hour at 4°C with rotation. During antibody binding, Protein A Dynabeads
711 (Invitrogen, 100 μL per sample) was washed three times with 900 μL beads wash buffer 1
712 (150 mM KCl, 5 mM $MgCl_2$, 10 mM HEPES [pH 7.4], 0.05% BSA (wt/vol), 1% NP-40). After
713 antibody binding, the mixture was added to the washed beads and gently mixed, followed
714 by incubation for 1 hour at 4°C with rotation. After incubation, the RNA-bound beads were
715 washed four times with 700 μL beads wash buffer 2 (RNase-free water containing 350 mM
716 KCl, 5 mM $MgCl_2$, 10 mM HEPES [pH 7.4], 1% NP-40, 2 mM DTT, 100 U/mL recombinant

717 RNasin (Promega), 100 μg/mL cycloheximide, 5 mM sodium fluoride, 1 mM sodium
718 orthovanadate, 1 mM sodium pyrophosphate, 1 mM beta-glycerophosphate). During the
719 final wash, beads were placed onto the magnet and moved to room temperature. After
720 removing supernatant, RNA was eluted by mixing the beads with 350 μL RLT (Qiagen). The
721 eluted RNA was purified using RNeasy Micro kit (Qiagen). Chemicals were purchased from
722 Sigma if not specified otherwise.
723 cDNA from purified RNA were generated using SMART-Seq v4 Ultra Low Input RNA Kit
724 (Takara Clontech). Libraries were made using the Nexterra XT DNA Library Preparation
725 Kit. Up to 12 samples were pooled and sequenced on Illumina HiSeq2000/2500 on single-
726 end read mode. RNA-Seq data was aligned using Kallisto. Differential expression analysis
727 was performed using a combination of DESeq and EdgeR packages in R.
728

729 **Open-field behavior test**

730

731 The behavior of the mice was observed on post-surgery days 1 and 3. Three groups of
732 mice were observed, *i.e.*, the no-injury control group, the Oil control group, and the BCP
733 group. The no-injury control group had the dorsal hair removed and a bandage was placed
734 on the day when other mice went through surgeries, but no incision was made. Bandages of
735 these mice were changed daily as well. The olive oil control group and the BCP group
736 underwent the procedure detailed above. A mouse was placed in a cup (about 10 cm
737 diameter x 15 cm height) and placed in the center of an open field test apparatus
738 (measurements: width 50 cm x depth 25 cm x height 30 cm) covered with the cup. Video

recording using a camera (Logitech QuickCam Pro9000) and bTV software was conducted either from the top for analysis of the amount of traveling or from the side for analysis of behavior patterns. After camera was started, the cup covering the mouse was removed and behaviors were recorded for 5 minutes. The behaviors recorded from the top were analyzed using Ethovision (Version 7, Noldus, Leesburg, VA) and behaviors recorded from the side were analyzed using ELAN software (http://tla.mpi.nl/tools/tla-tools/elan/, Max Planck Institute for Psycholinguistics, The Language Archive, Nijmegen, The Netherlands) [87]. Behaviors were categorized based on the definition given by previous studies [88-90] and quantified using ELAN software. The behaviors coded using ELAN were then exported to Microsoft Excel where average time for each behavior, incidence of each behavior, and total time for each behavior were determined.

Statistical analyses

ANOVA and Student T-tests were used for comparison of the groups. Tukey post-hoc test was used for pair-wise comparison. Comparison of % was conducted using Fisher's exact test of indepence.

Acknowledgements

This project was funded by the Office of the Vice Provost of Research at Indiana University Bloomington through the Collaborative Research and Creative Activity Funding Award to S.K. while she was Associate Research Professor at the Medical Science Program of the School of Medicine of IU. Large amount of this project was conducted while S.K. was Associate Research Professor at the Medical Science Program of the School of Medicine of

762 IU, financially supported by the previous Director of Medical Science Program, Prof. John
763 Watkins III. S.K. thanks Dr. A. Poehlman for her help in editing English. S.K thanks A.
764 Straiker of the Department of Psychological and Brain Sciences, IU, for his kind gift of CB2
765 agonist and antagonist used in the project and also for the advice on CB2. S.K thanks J.
766 Wager-Miller of the Department of Psychological and Brain Sciences, IU, for his kind gift of
767 CB2 knockout mice in the project. S.K. thanks J. Foley of Medical Science Program of IU
768 School of Medicine to let S.K. use part of his laboratory space and resources for the project.
769 S.K. thanks S. Childless of Medical Science Program of IU School of Medicine for her help in
770 sectioning samples and J.K. Leffel II of Department of Psychological and Brain Sciences, IU,
771 for his help on using Ethovision. RNA sequencing and bioinformatic analyses was
772 conducted at the Center for Genomics and Bioinformatics of IUB and S.K. thanks A.M.
773 Buechlein, D.B. Rusch and J. Huang for their services. S.K. also thanks K. Mackie of the
774 Department of Psychological and Brain Sciences for his advice on the project, J. Powers of
775 the IU Light Microscopy Imaging Center (LMIC) for his help and advice while using LMIC,
776 and D. Sinkiewicz of the Center for the Integrative Study of Animal Behavior Laboratory
777 (CISAB Lab) for advice. S.K. thanks the staff of laboratory animal resources (LAR) of IU for
778 their assistance in maintaining her mice colony.
779

780 # References

781 1. Koyama S. Primer Effects by Murine Pheromone Signaling. Pheromonal Influences
782 on Reproductive Conditions. Springer International Publishing AG, Vienna: Springer
783 Briefs in Animal Sciences, Springer; 2016.

784 2. Kim JT, Ren CJ, Fielding GA, Pitti A, Kasumi T, Wajda M, Lebovits A, Bekker A.
785 Treatment with lavender aromatherapy in the post-anesthesia care unitreduces
786 opioid requirements of morbidly obese patients undergoing laparoscopic adjustable
787 gastric banding. Obes Surg. 2007;17(7): 920-925.
788 3. Marzouk T, Barakat R, Ragab A, Badria F, Badawy A. Lavender-thymol as a new
789 topical aromatherapy preparation for episiotomy: a randomized clinical trial. J
790 Obstet Gynaecol. 2015;35(5): 472-475.
791 4. Malcolm BJ, Tallian K. Essential oil of lavender in anxiety disorders: ready for prime
792 time? Ment Health Clin. 2017;7(4): 147-155.
793 5. Nasiri A, Mahmodi MA. Aromatherapy massage with lavender essential oil and the
794 prevention of disability in ADL in patients with osteoarthritis of the knee: a
795 randomized controlled clinical trial. Complement Ther Clin Pract. 2018;30: 116-121.
796 6. Schneider R, Singer N, Singer T. Medical aromatherapy revisited- basic mechanisms,
797 critique, and a new development. Hum Psychopharmacol Clin Exp. 2019;34: e2683.
798 7. Mazutti d Silva SM, Rezende Costa CR, Gelfuso GM, Silva Guerra EN, de Medeiros
799 Nobreg YK. Et al. Wound healing effect of essential oil extracted from *Eugenia*
800 *dysenterica* DC (Myrtaceae) leaves. Molecules. 2019; 24: 2.
801 8. Tanbirul Haque ASM, Moon JN, Saravana PS, Tilahun A, Chun B-S. Composition of
802 *Asarum heterotropoides var. mandshuricum* radix oil from different extraction
803 methods and activities against human body odor-producing bacteria. J Food Drug
804 Anal. 2016; 24(4): 813-821.

805 9. El-Jalel LFA, Elkady WM, Gonaid MH, El-Gareeb KA. Differences in chemical
806 composition and antimicrobial activity of *Thymus capitatus* essential oil at different
807 altitudes. Future J. Pharm Sci. 2018; 4(2): 156-160.
808 10. Lee L-S, Kim S-H, Kim Y-B, Kim Y-C. Quantitative analysis of major constituents in
809 green tea with different plucking periods and their antioxidant activity. Molecules.
810 2014; 19: 9173-9186.
811 11. Chamorro ER, Ballerini G, Sequeira AF, Velasco GA, Zalazar MF. Chemical
812 composition of essential oil from *Tagetes minuta L*. leaves and flowers. J. Argentine
813 Chem Soc. 2008; 96(1-2): 80-86.
814 12. Lis A, Swaczyna A, Krajewska A, Mellor K. Chemical composition of the essential oils
815 from twigs, leaves, and cones of Thuja plicata and its cultivar varieties "fastigiata",
816 "kornik," and "zebrina". Nat. Prod. Comm. 2019; 2019: 1-5.
817 13. Ma D-L, Chan DS-H, Wei G, Zhong H-J, Yang H. et al. Virtual screening and
818 optimization of Type II inhibitors of JAK2 from a natural product library. Chem.
819 Commun. 2014; 50: 13885-13888.
820 14. Yang C, Wang W, Chen L, Liang J, Lin S. et al. Discovery of a VHL and HIF1alpha
821 interaction inhibitor with in vivo angiogenic activity via structure-based virtual
822 screening. Chem. Comm. 2016; 52:12837-12840.
823 15. Khazneh E, Hribova P, Hosek J, Suchy P, Kollar P. et al. The chemical composition of
824 *Achillea wilhelmsii* C. Koch and its desirable effects on hyperglycemia, inflammatory
825 mediators and hypercholesterolemia as risk factors for cardiometabolic disease.
826 Molecules. 2016; 21(4): 404.

827 16. Yu SH, Seol GH. *Lavandula angustifolia* Mill. Oil and its active constituent linalyl
828 acetate alleviate pain and urinary residual sense after colorectal cancer surgery: a
829 randomised controlled trial. Evid. Based Complement. Alternat. Med. 2017; 2017:
830 3954181.
831 17. de Freitas Souza C, Descovi S, Baldissera MD, Bertolin K, Bianchini AE. et al.
832 Involvement of HPI-axis in anesthesia with *Lippia alba* essential oil citral and
833 linalool chemotypes: gene expression in the secondary responses in silver catfish.
834 Fish Physiol. Biochem. 2019; 45(1): 155-166.
835 18. Kang N, Koo J. Olfactory receptors in non-chemosensory tissues. BMB Rep.
836 2012;45(11): 612-622.
837 19. Chen Z, Zhao H, Fu N, Chen L. The diversified function and potential therapy of
838 ectopic olfactory receptors in non-olfactory tissues. J Cell Physiol. 2018;233(3):
839 2104-2115.
840 20. Gertsch J, Leonti M, Raduner S, Racz I, Chen JZ, Xie XQ, Altmann K-H, Karsak M,
841 Zimmer A. Beta-caryophyllene is a dietary cannabinoid. Proc Natl Acad Sci USA.
842 2008;105: 9099-9104.
843 21. Zheng JL, Yu TS, Li XN, Fan YY, Ma WX, Du Y, Zhao R, Guan D-W. Cannabinoid
844 receptor type 2 is time-dependently expressed during skin wound healing in mice.
845 Int J Legal Med. 2012;126(5): 807-814.
846 22. Li SS, Wang LL, Liu M, Jiang SK, Zhang M, Tian ZL, Wang M, Li J-Y, Zhao R, Guan D-W.
847 Cannabinoid CB2 receptors are involved in the regulation of fibrogenesis during
848 skin repair in mice. Mol Med Rep. 2016;13(4): 3441-3450.

849 23. Wang LL, Zhao R, Li JY, Liu M, Wang M, Zhang MZ, Dong W-W, Jiang S-K, Xhang M,
850 Tian Z-L, Liu C-S, Guan D-W. Pharmacological activation of cannabinoid 2 receptor
851 attenuates inflammation, fibrogenesis and promotes re-epithelialization during skin
852 wound healing. Eur J Pharmacol. 2016;786: 128-136.
853 24. Amorim JL, Figueiredo JB, Amaral ACF, Barros EGO, Pelmero C, MPalantinos MA,
854 Ramos AdS, Ferreira JLP, Silva JRdA, Benjamim CF, Basso SL, Nasciutti LE, Fernandes
855 PD. Wound healing properties of *Copaifera paupera* in diabetic mice. PloS One.
856 2017;12(10): e0187380.
857 25. Gonzalez AC, Costa TF, Andrade ZA, Medrado AR. Wound healing – A literature
858 review. An Bras Dermatol. 2016;91(5): 614-620.
859 26. Landen NX, Li D, Stahle M. Transition from inflammation to proliferation: a critical
860 step during wound healing. Cell Mol Life Sci. 2016;73: 3861-3885.
861 27. Rittie L. Cellular mechanisms of skin repair in humans and other animals. J Cell
862 Commun Signal. 2016;10: 103-120.
863 28. Sorg H, Tilkorn DJ, Hager S, Hauser J. Skin wound healing: an update on current
864 knowledge and concepts. Eur Surg Res. 2017;58(1-2): 81-94.
865 29. Braiman-Wiksman L, Solomonik I, Spira R, Tennenbaum T. Novel insights
866 into wound healing sequence of events. Toxicol Pathol. 2007; 35: 767-779.
867 30. Tracy LE, Minasian RA, Caterson EJ. Extracellular matrix and dermal fibroblast
868 function in the healing wound. Adv Wound Care (New Rochelle). 2016; 5(3): 119-
869 136.
870 31. Kezic S, Jakasa I. Filaggrin and skin barrier function. Curr Probl Dermatol. 2016; 49:
871 1-7.

872 32. Ashcroft GS, Dodsworth J, van Boxtel E, Tarnuzzer RW, Horan MA, Schultz GS,
873 Ferguson MWJ. Estrogen accelerates cutaneous wound healing associated with an
874 increase in TGF-beta1 levels. Nat Med. 1997;3(11): 1209-1215.
875 33. Heldin CH, Westermark B. Mechanism of action and in vivo role of platelet-derived
876 growth factor. Physiol Rev. 1999; 79(4): 1283-1316.
877 34. Horikawa S, Ishii Y, Hamashima T, Yamamoto S, Mori H, Fujimori T, Shen J, Inoue R,
878 Nishizono H, Itoh H, Majima M, Abraham D, Miyawaki T, Sasahara M. PDGFRα plays
879 a crucial role in connective tissue remodeling. Sci Rep. 2016; 5:17948. Doi:
880 10.1038/Srep17948.
881 35. Ivaska J, Pallari HM, Nevo J, Eriksson JE. Novel functions of vimentin in cell adhesion,
882 migration, and signaling. Exp Cell Res. 2007; 313(10): 2050-2062.
883 36. Cheng F, Shen Y, Mohanasundaram P, Lindstrom M, Ivaska J, Ny T, Eriksson JE.
884 Vimentin coordinates fibroblast proliferation and keratinocyte differentiation in
885 wound healing via TGF-β-slug signaling. Proc Natl Acad Sci U S A. 2016; 113(30):
886 E4320-4327.
887 37. Solanas, G., Benitah, S.A. Regenerating the skin: a task for the heterogeneous stem
888 cell pool and surrounding niche. Nat Rev Mol Cell Biol 2013; 14: 737-748.
889 38. Kretzschmar, K., Watt, F.M. Markers of epidermal stem cell subpopulations in adult
890 mammalian skin. Cold Spring Harb Perspect Med 2014; 4: a013631.
891 39. Watt, F.M. Mammalian skin cell biology: At the interface between laboratory and
892 clinic. Science 2014; 346: 937-940.

893 40. Aragona M, Dekoninck S, Rulands S, Lenglez S, Mascre G, Simons BD, Blanpain C.
894 Defining stem cell dynamics and migration during wound healing in mouse skin
895 epidermis. Nat Comm. 2017;8: Article number 14684.
896 41. Ito, M., Liu, Y., Yang, Z., Nguyen, J., Liang, F., Morris, R.J., Cotsarelis, G. Stem cells in
897 the hair follicle bulge contribute to repair but not to homeostasis of epidermis. Nat
898 Med 2005; 11: 1351-1354.
899 42. Pertwee R, Griffin G, Fernando S, Li X, Hill A, Makriyannis A. AM630, a competitive
900 cannabinoid receptor antagonist. Life Sci. 1995; 56(23-24): 1949-1955.
901 43. Huffman, JW. CB2 receptor ligands. Mini Rev Med Chem. 2005; 5(7): 641-649.
902 44. Wu DD, Inwin DM, Zhang YP. Molecular evolution of the keratin associated protein
903 gene family in mammals, role in the evolution of mammalian hair. BMC Evol Biol.
904 2008; 8: 241. Doi: 10.1186/1471-2148-8-241.
905 45. Fujikawa H, Fujimoto A, Farooq M, Ito N, Shimomura Y. Characterization of the
906 human hair keratin-associated protein 2 (KRTAP2) gene family. J Invest Dermatol.
907 2012;132: 1806-1813
908 46. Kuno K, Kanada N, Nakashima E, Fujiki F, Ichimura F, Matsushima K. Molecular
909 cloning of a gene encoding a new type of metalloproteinase-disintegrin family
910 protein with thrombospondin motifs as an inflammation associated gene. J Biol
911 Chem. 1997; 272(1): 556-562.
912 47. Grotewold L, Plum M, Dildrop R, Peters T, Ruther U. Bambi is coexpressed with
913 Bmp-4 during mouse embryogenesis. Mech Dev. 2001; 100(2): 327-330.
914 48. Liu YH, Ma L, Wu LY, Luo W, Kundu R, Sangiorgi F, Snead ML, Maxson R. Regulation
915 of the Msx2 homeobox gene during mouse embryogenesis: a transgene with 439 bp

916 of 5' flanking sequence is expressed exclusively in the apical ectodermal ridge of the
917 developing limb. Mech Dev. 1994; 48(3): 187-197.
918 49. Morasso MI, Markova NG, Sargent TD. Regulation of epidermal differentiation by a
919 Distal-less homeodomain gene. J Cell Biol. 1996; 135(6 Pt 2): 1879-1887.
920 50. Dong S, Yng S, Kojima T, Shiraiwa M, Kawada A, Mechin MC, Adoue V, Chavanas S,
921 Serre G, Simon M, Takahara H. Crucial roles of MZF1 and Sp1 in the transcriptional
922 regulation of the peptidylarginine deiminase type I gene (PADI1) in human
923 keratinocytes. J Invet Dermatol. 2008; 128(3): 549-557.
924 51. Jave-Suarez LF, Winter H, Langbein L, Rogers MA, Schweizer J. HOXC13 is involved
925 in the regulation of human hair keratin gene expression. J Biol Chem. 2002; 277(5):
926 3718-3726.
927 52. Breen EC, Tang K. Calcyclin (S100A6) regulates pulmonary fibroblast proliferation,
928 morphology, and cytoskeletal organization in vitro. J Cell Biochem. 2003; 88(4):
929 848-854.
930 53. Kondo T, Ohshima T. The dynamics of inflammatory cytokines in the healing process
931 of mouse skin wound: a preliminary study for possible wound age determination.
932 Int J Legal Med. 1996; 108: 231-236.
933 54. St Laurent G III, Seilheimer B, Tackett M, Zhou J, Shtokalo D. Vyatkin Y, Ri M, Toma I,
934 Jones D, McCaffrey TA. Deep sequencing transcriptome analysis of murine wound
935 healing: effects of a multicomponent, multitarget natural product therapy-Tr14.
936 Front Mol Biosci. 2017;17: https://doi.org/10.3389/fmolb.2017.00057.
937 55. Premkumar LS. Transient receptor potential channels as targets for phytochemicals.
938 ACS Chem Neurosci. 2014; 5(11): 1117-1130.

939 56. Caterina MJ. TRP channel cannabinoid receptors in skin sensation, homeostasis, and
940 inflammation. ACS Chem Neurosci. 2014; 5(11): 1107-1116.
941 57. Premkumar LS, Abooj M. TRP channels and analgesia. Life Sci. 2013; 92(8-9): 415-
942 424.
943 58. Colonna M, Facchetti F. TREM-1 (triggering receptor expressed on myeloid cells): a
944 new player in acute inflammatory responses. J Infect Dis. 2003; 187 Suppl 2: S397-
945 401.
946 59. Johnson RL, Riddle RD, Laufer E, Tabin C. Sonic hedgehog: a key mediator of
947 anterior-posterior patterning of the limb and dorso-ventral patterning of axial
948 embryonic structures. Biochem Soc Trans. 1994; 22(3): 569-574.
949 60. Eaton S. Planar polarization of drosophila and vertebrate epithelia. Curr Opin Cell
950 Biol. 1997; 9(6): 880-886.
951 61. Maddaluno L, Urwyler C, Werner S. Fibroblast growth factors: key players in
952 regeneration and tissue repair. Development, 2017; 144(22): 4047-4060.
953 62. MacDonald BT, Tamai K, He X. Wnt/beta-catenin signaling: components,
954 mechanisms, and diseases. Dev Cell. 2009; 17(1): 9-26.
955 63. Abe, Y., Tanaka, N. Roles of hedgehog signaling pathway in epidermal and hair
956 follicle development, homeostasis, and cancer. J Dev Biol 2017; 5: E12 doi:
957 10.3390/jdb5040012.
958 64. Brownell, I. Guevara, E., Bai, C.B., Loomis, C.A., Joyner, A.L. Nerve-derived sonic
959 hedgehog defines a niche for hair follicle stem cells capable of becoming epidermal
960 stem cells. Cell Stem Cell 2011; 8(5): 552-565.

961 65. Caddy, J., Wilanowski, T., Darido, C., Dworkin, S., Ting, S.B. Zhao Q, Rank G, Auden A,
962 Srivastava S, Papenfuss TA, Murdoch JN, Humbert PO, Boulos N, Weber T, Zuo J,
963 Cunningham JM, Jane SM. Epidermal wound repair is regulated by the planar cell
964 polarity signaling pathway. Dev Cell 2010; 19(1): 138-147.
965 66. Bayly, R., Axelrod, J.D. Pointing in the right direction: new developments in the field
966 of planar cell polarity. Nat Rev Genet 2011; 12(6): 385-391.
967 67. Munoz-Soriano, V., Belacortu, Y., Paricio, N. Planar cell polarity signaling in collective
968 cell movements during morphogenesis and disease. Curr Genomics 2012; 13(8):
969 609-622.
970 68. Richardson, R., Metzger, M., Knyphausen, P., Ramezani, T., Slanchev, K., Kraus, C.,
971 Schmelzer, E., Hammerschmidt, M. Re-epithelialization of cutaneous wounds in
972 adult zebrafish combines mechenisms of wound closure in embryonic and adult
973 mammals. Development 2016; 143: 2077-2088.
974 69. Azzi L, El-Alfy M, Martel C, Labrie F. Gender differences in mouse skin morphology
975 and specific effects of sex steroids and dehydroepiandrosterone. J. Invest. Dermatol.
976 2005;124(1): 22-27.
977 70. Ashcroft GS, Mills SJ. Androgen receptor-mediated inhibition of cutaneous wound
978 healing. J Clin Invest. 2002;110(5), 615-624.
979 71. Gilliver SC, Ashcroft GS. Sex steroids and cutaneous wound healing: the contrasting
980 influences of estrogens and androgens. Climacteric. 2007;10(4) 276-288.
981 72. Busse D, Kudella P, Gruening NM, Gisselmann G, Stander S, Luger T, Jacobsen F,
982 Steinstrasser L, Paus R, Gkogkolou P, Bohm M, Hatt H, Benecke H. A synthetic

983 sandalwood odorant induces wound-healing processes in human keratinocytes via
984 the olfactory receptor OR2AT4. J Invest Dermatol. 2014;134(11): 2823-2832.
985 73. Harada H, Kashiwadani H, Kanmura Y, Kuwaki T. Linalool odor-induced anxiolytic
986 effects in mice. Front Behav Neurosci. 2018;12: 241 doi:
987 10.3389/fnbeh.2018.00241.
988 74. Jiang Y, Gong NN, Hu XS, Ni MJ, Pasi R, Matsunami H. Molecular profiling of activated
989 olfactory neurons identifies odorant receptors for odors *in vivo*. Nat Neurosci.
990 2015;18: 1446-1454.
991 75. Sicard G, Holley A. Receptor cell responses to odorants: similarities and differences
992 among odorants. Brain Res. 1985;292: 283-296.
993 76. Fleischer J, Breer H, Strotmann J. Mammalian olfactory receptors. Front Cell
994 Neurosci. 2009;3: 9. Doi: 10.3389/neuro.03.009.2009.
995 77. Mahmoud MF, Swefy SE, Hasan RA, Ibrahim A. Role of cannabinoid receptors in
996 hepatic fibrosis and apoptosis associated with bile duct ligation in rats. Eur J
997 Pharmacol. 2014;742: 118-124.
998 78. Yang M, Lv Y, Tian X, Lou J, An R, Zhang Q, Li M, Dong Z. Neuroprotective effect of β-
999 caryophyllene on cerebral ischemia-reperfusion injury via regulation of necroptotic
1000 neuronal death and inflammation: In vivo and in vitro. Front. Neurosci. 2017;11:
1001 583.
1002 79. Fuchs, Y., Brown, S., Gorenc, T., Rodriguez, J., Fuchs, E., Steller, H. *Sept4*/ARTS
1003 regulates stem cell apoptosis and skin regeneration. Science 2013; 341: 286-289.
1004 80. Wilgus TA, Bergdall VK, DiPietro LA, Oberyszyn TM. Hydrogen peroxide disrupts
1005 scarless fetal wound repair. Wound Repair Regen. 2005;13(5): 513-519.

1006 81. Mescher AL. Macrophages and fibroblasts during inflammation and tissue repair in
1007 models of organ regeneration. Regeneration. 2017;4: 39-53.
1008 82. Vanderhaeghen P, Schurmans S, Vassart G, Parmentier M. Olfactory receptors are
1009 displayed on dog mature sperm cells. J Cell Biol. 1993;123(6 Pt1): 1441-1452.
1010 83. Vosshall LB. Olfaction: attracting both sperm and the nose. Curr Biol. 2004;14(21):
1011 R918-920.
1012 84. Adams RP. Identification of essential oil components by gas chromatography/
1013 quadrupole mass spectroscopy. Carol Streams: Allured Publishing Corporation;
1014 2001.
1015 85. Jemiolo B, Harvey S, Novotny M. Promotion of the Whitten effect in female mice by
1016 synthetic analogs of male urinary constituents. Proc Natl Acad Sci USA. 1986;83(12):
1017 4576-4579.
1018 86. Harvey S, Jemiolo B, Novotny M. Pattern of volatile compounds in dominant and
1019 subordinate male urine. J Chem Ecol. 1989;15(7): 2061-2072.
1020 87. Lausberg H, Sloetjes H. Coding gestural behavior with NEUROGES—ELAN system.
1021 Behav Res Methods. 2009;41(3): 841-849.
1022 88. Grant EG, Mackintosh JH. A comparison of the social posture of common laboratory
1023 rodents. Behaviour, 1963;21: 247-259.
1024 89. Wilson RC, Vacek T, Lanier DL, Dewsbury DA. Open-field behavior in muroid
1025 rodents. Behav Biol. 1976;17: 495-506.
1026 90. Weyers P, Janke W, Macht M, Weijers HG. Social and non-social open field
1027 behaviours of rats under light and noise stimulation. Behav Processes. 1994;31:
1028 257-268.

1029 91. Sköld M, Karlberg AT, Matura M, Börje A. The fragrance chemical beta-
1030 caryophyllene-air oxidation and skin sensitization. Food Chem Toxicol. 2005;44:
1031 538-545.
1032 92. Kalueff AV, Tuohimaa P. Grooming analysis algorithm for neurobehavioural stress
1033 research. Brain Res Brain Res Protoc. 2004;13(3): 151-158.
1034 93. Smolinsky AN, Bergner CL, LaPorte JL, Kalueff AV. Analysis of grooming behavior
1035 and its utility in studying animal stress, anxiety, and depression. In: Gould TD,
1036 editor. Mood and Anxiety Related Phenotypes in Mice, Neuromethods 2017,42, DOI
1037 10.1007/978-1-60761-303-9_2, © Humana Press.
1038

1039 **Author contributions:** S.K conceptualized and led the study. S.K., A.P., and M.K. performed
1040 the *in vivo* mouse experiments. S.K. performed all the *in vitro* assays. H.M. conducted pS6-
1041 IP RNA-Seq experiments. A.M. analyzed the results of RNA sequencing, read the
1042 manuscript, and discussed with S.K. while finalizing it as a paper. K.D. and C.K. edited the
1043 manuscript and provided important comments on the organization and experimental
1044 approaches. H.A.S. and M.V.N. prepared SBT solution and analyzed the BCP from Sigma-
1045 Aldrich, read and edited the manuscript. S.K. wrote the manuscript with input from other
1046 authors.
1047

1048 Supporting information

1049 **S1 Fig. Reservoir to hold treatment media.** Small (5 mm x 5 mm) full-thickness excisions
1050 were made on the backs of adult mice and methods to hold the treatment buffer solution on
1051 the wounded area were developed. A silicone ring, which held 50 μL of buffer solution, was

1052 attached to the wounded area using a liquid sealing bandage (center). After the buffer
1053 solution was placed in the ring, a transparent lid made of polydimethylsiloxane (PDMS)
1054 was installed on top of the ring and was then sealed with the liquid sealing bandage (center
1055 and upper right). A gauze bandage was used to cover the body to prevent the mouse from
1056 removing the ring (lower right). (141 words)
1057
1058 **S2. Fig. Behavioral patterns observed by BCP, Oil, and NT group.** A concern in the use
1059 of BCP is that it may cause allergic responses. An oxidation product of BCP, *i.e.*,
1060 caryophyllene oxide, is known as mild allergen [91]. To examine whether BCP has side
1061 effects, we conducted open-field tests on post-surgery day 1 (PS1) and 3 (PS3) and
1062 conducted behavioral analyses, specifically focusing on behavior patterns including
1063 scratching behaviors as an evidence of sensitization. In figures, NT group mice are mice
1064 without skin excision but went through all other steps and kept bandage on the same time
1065 length. There was almost no incidence of scratch behaviors on post-surgery day 1 **(a)** nor
1066 on post-surgery day 3 **(b)**. Statistically significant differences were found in self-grooming
1067 behaviors of post-surgery day 3 (ANOVA, $F_{2,15}$=4.585, P=0.028). Self-grooming behaviors
1068 are known to increase at both high and low stress situations [92, 93]. If there are
1069 differences in the way BCP group mice did self-grooming behaviors, it could be due to BCP
1070 treatment. We classified self-grooming behaviors by the part in the body they groom and
1071 called them Phase 1 to Phase 4 following earlier studies [92, 93], and analyzed the self-
1072 grooming behaviors. We found no differences among the groups in the way self-grooming
1073 behaviors was conducted on both post-surgery day 1 and 3 (S2 Fig c,d), which suggest that
1074 BCP treatment did not cause mice to self-groom in a different way. **(c)** and **(d)** show the %

1075 of short to long, full sequences of self-grooming behaviors depending on the group on post-
1076 surgery day 1 **(c)** (NT, n=6, Oil, n=6, BCP, n=7) and 3 **(d)** (NT, n=6, Oil n=5, BCP, n=7).
1077 Classification of self-grooming behavior is as follows [92, 93]: around the nose area (Phase
1078 I), around the face (Phase II), around the head and ears (Phase III), and to the body (Phase
1079 IV). Groomings toward the bandage were excluded from Phase IV to avoid the possibility
1080 that these grooming could be intention to remove bandages. Each incidence of grooming
1081 was classified into the number of phases they include and % of short self-groomings
1082 (include only one phase) to long full self-groomings (include four phases) were calculated
1083 to determine if BCP group showed shorter self-groomings as signs of irritation stress.
1084 The % of self-grooming with four phases was higher in the BCP group but there were no
1085 statistically significant differences among groups. Based on these differences in the amount
1086 of self-grooming behaviors, we examined the travel distances and velocity of movements
1087 when they move and found that BCP group showed less travel distance and slower velocity
1088 (S3 Fig). (285 words)
1089
1090 **S3. Fig. Distance traveled and velocity of movements in BCP, Oil, and NT group mice**.
1091 Open-field analyses of traveling distances and moving velocity revealed that on post-surgery
1092 day 1, there were no statistically significant differences among groups in the distance traveled
1093 **(a)** and velocity of movements **(b)** (ANOVA, distance, $F_{2,21}$=2.205, P=0.135; velocity,
1094 $F_{2,21}$=2.647, P=0.094; NT, n=6, Oil, n=6, BCP, n=7). On post-surgery day 3, the distance
1095 traveled **(c)** was significantly shorter and the velocity was significantly slower **(d)** in the BCP
1096 group, whereas there were no differences between the Oil group and NT group (ANOVA,
1097 distance, $F_{2,9}$=9.113, P=0.007; velocity, $F_{2,9}$=9.495, P=0.006; NT, n=6, Oil n=5, BCP, n=7).

1098 Linalool, a chemical compound included in lavender extracts, has anxiolytic effect in mice
1099 [68]. Whether the slower movements and increased self-grooming are signs that BCP has
1100 anxiolytic influence like linalool need to be addressed in future. Overall, these results
1101 showed that the impact of BCP on behavior was the longer time staying at a place doing
1102 self-grooming and the slow movements when the mice walked, which contain no signs of
1103 irritation from allergic responses. The BCP we used contains only 1.6% of caryophyllene
1104 oxide (S4 Fig., S1 Table) and fresh BCP was applied daily. The daily change may have
1105 contributed to reduce sensitization and allergic reactions. (346 words)
1106
1107 **S4 Fig. Beta-caryophyllene standard (Sigma-Aldrich) composition/GC-MS.** 1:
1108 cubebene, 2, 4, 5, 7, 8: sesquiterpenes of MW 204, 3: copaene, 6: BCP, 9: neoclovene, 10: α-
1109 caryophyllene, 11: 9-epi(E)-caryophyllene, 12: caryophyllene oxide. See **S2 Table** for
1110 details. (39 words)
1111
1112 **S5 Fig. Results of RNA sequencing of post-surgery 17 hours skin and intact skin:**
1113 **Comparison between BCP and NT (a) and Oil and NT (b).** Heatmap showing the top 50
1114 significant gene expressions in the skin exposed to BCP (n=2) or oil (n=3), 17 to 18 hours
1115 post-surgery (inflammation stage), and in the skin of mice without skin excision (NT
1116 group) (n=3).
1117
1118 **S6 Fig. Influence of exposure to BCP on TREM1 pathway.** TREM1 signaling pathway
1119 showing the genes/groups of genes up-regulated (pink) and down-regulated (green) in
1120 BCP group compared to oil group. (28 words)

1121

1122 **S7 Fig. Signaling pathways showing the genes/groups of genes up-regulated (pink) in**

1123 **BCP group compared to oil group**. **(a)** Sonic hedgehog signaling (shh) pathway, **(b)**

1124 planar cell polarity (PCP) signaling pathway, **(c)** fibroblast growth factor (FGF) signaling

1125 pathway, and **(d)** Wnt beta-catenin signaling pathway. (42 words)

1126

1127 **S8 Fig. cfos expression in the olfactory bulb of mice exposed to BCP or SBT. (a)**

1128 Location where cfos was expressed profoundly. B **(b)** To test if mice can smell BCP, intact

1129 mice were exposed to BCP (n=3) or male murine pheromone 2-sec-butyl-4,5-

1130 dihydrothiazole (SBT) (n=5) [61, 62] for 60 min and perfused. Olfactory bulb was

1131 harvested, and processed to determine c-fos protein expression. Mice exposed to BCP and

1132 SBT both showed c-fos expression in the olfactory bulb. **(c)** Numbers of cfos+ cells were not

1133 statistically significantly different between the mice exposed to SBT and BCP because of the

1134 large variance in the expression of cfos. The expression was high in the females at estrous

1135 stage. Error bars indicates sd of total number of cells. GL: glomerular layer, EPI: external

1136 plexiform layer, MI: mitral cell layer, IPI: internal plexiform layer, GR: granule cell layer.

1137 (141 words)

1138

1139 **S9 Fig. Influence of exposure to BCP through the olfactory system**. Mice were exposed

1140 to BCP or olive oil (Oil) through air by putting Q-tip soaked with either BCP or olive oil in a

1141 wire mesh and placing the wire mesh on top of the food provider **(a)**. Food was placed as

1142 much as possible to avoid the possibility that mice can reach to the wire mesh. Mice went

1143 through surgery and surgery area was covered by the ring reservoir filled with olive oil and

1144 sealed by PDMS lid, which was covered by a bandage. **(b)** Exposure to BCP through air did
1145 not differ from control level and significantly different from topical application of BCP
1146 (ANOVA, BCP vs Oil $F_{1,66}=15.803$, $P<0.001$, Topical vs Air $F_{1,66}=13.01$, $P=0.001$,
1147 Interaction $F_{1,66}=6.701$, $P=0.012$, BCP-Top, n=16, Oil-Top, n=16, BCP-Air, n=18, Oil-Air,
1148 n=20) ***: $P<0.001$, Tukey's pairwise comparison was used for pair wise comparison. (138
1149 words)
1150
1151 **S1 Table. Beta-caryophyllene standard (W225207, Sigma-Aldrich) composition/GC-**
1152 **MS**
1153
1154 **S2 Table. Olfactory receptor genes in the olfactory epithelium up-regulated after 1**
1155 **hour exposure to BCP**
1156
1157 **S3 Table. Olfactory receptors expressed in skin after exposure to BCP, compared**
1158 **with Oil group**
1159
1160

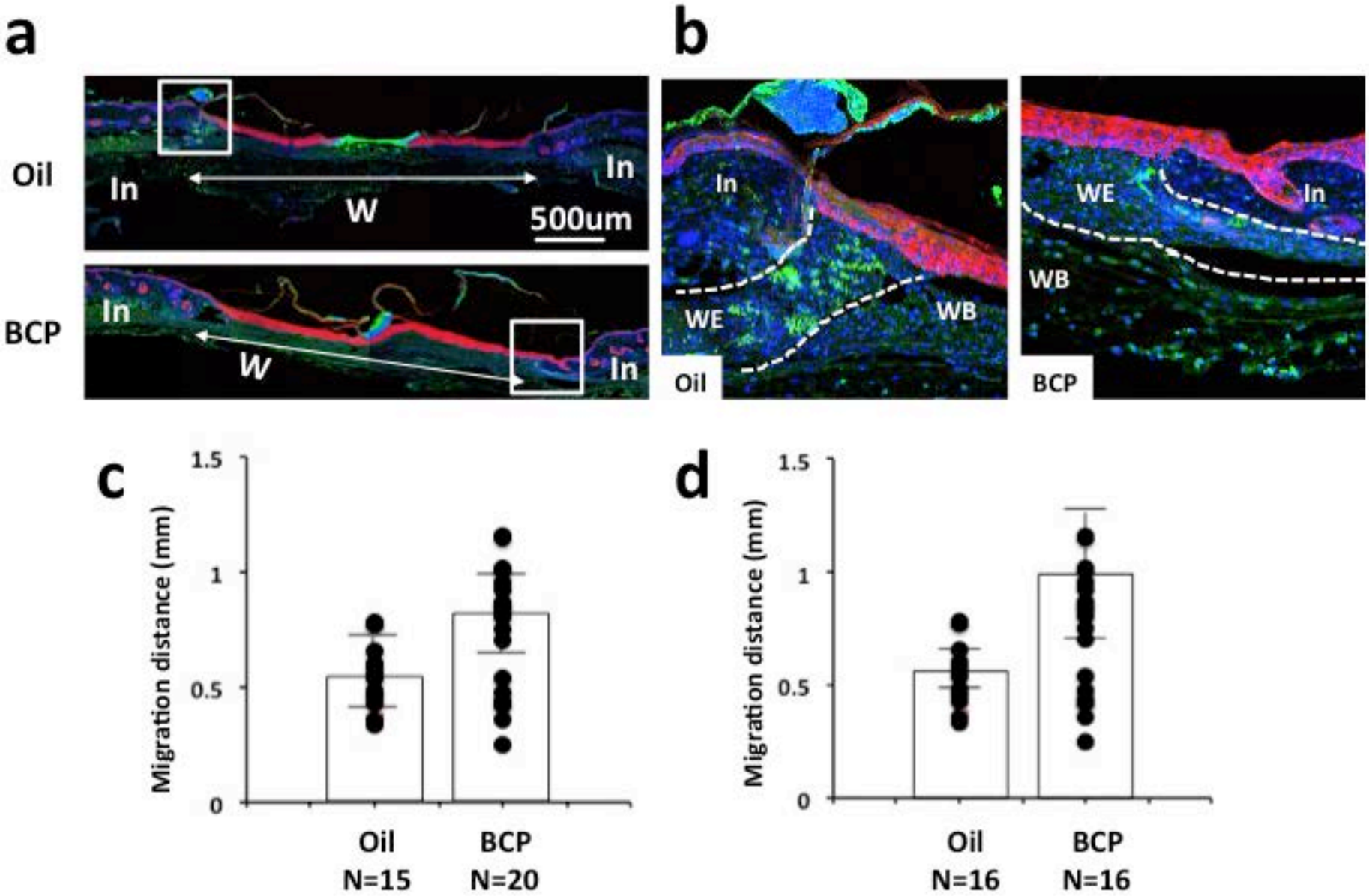
a
b
Oil
BCP
In
W
500um
WE
WB
c
d
Migration distance (mm)
1.5
1
0.5
0
Oil
N=15
BCP
N=20
Oil
N=16
BCP
N=16

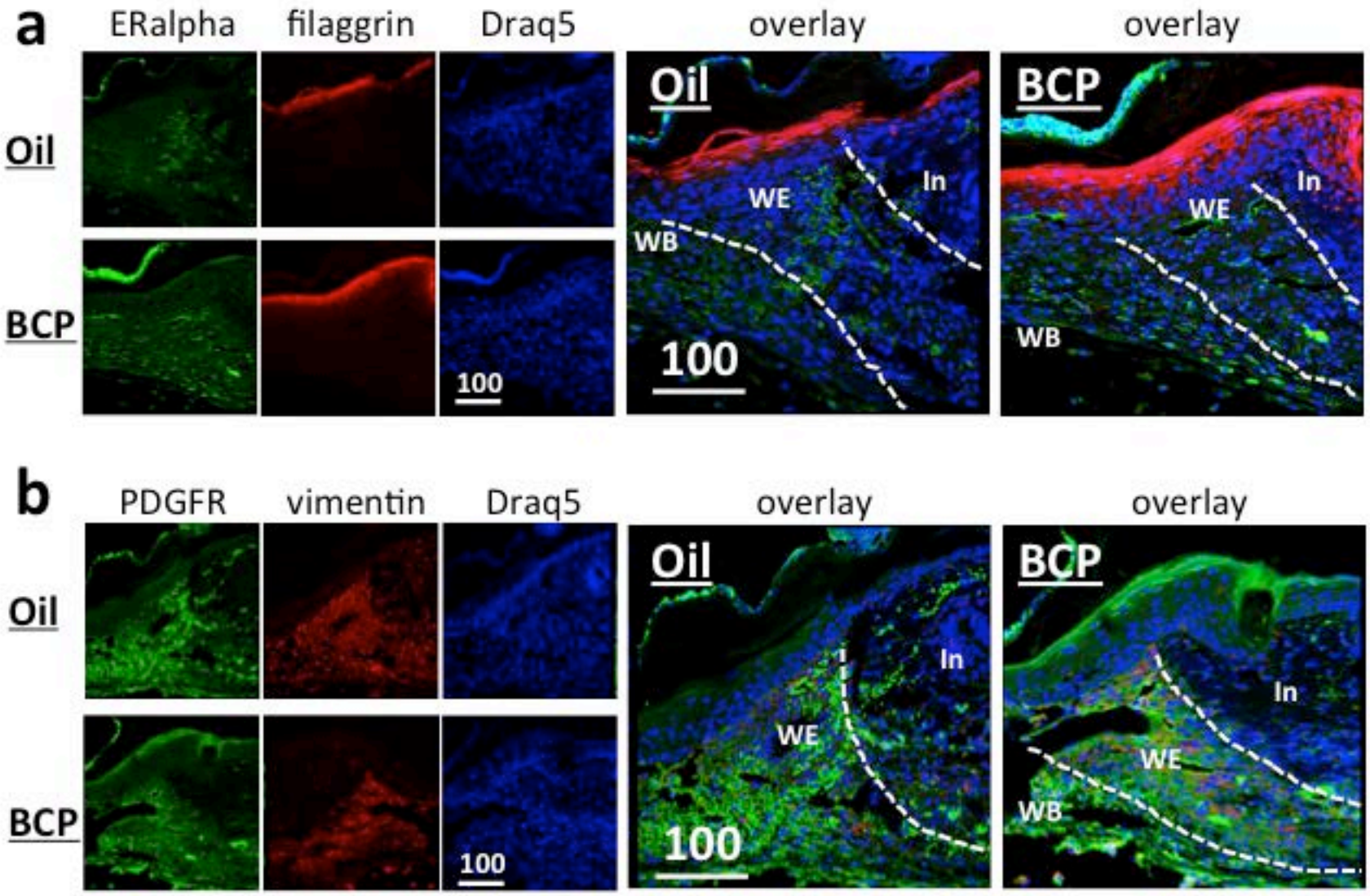
a
ERalpha
filaggrin
Draq5
overlay
overlay
Oil
BCP
Oil
WE
In
WB
100
BCP
WE
In
WB
100
b
PDGFR
vimentin
Draq5
overlay
overlay
Oil
BCP
Oil
In
WE
100
BCP
In
WE
WB
100

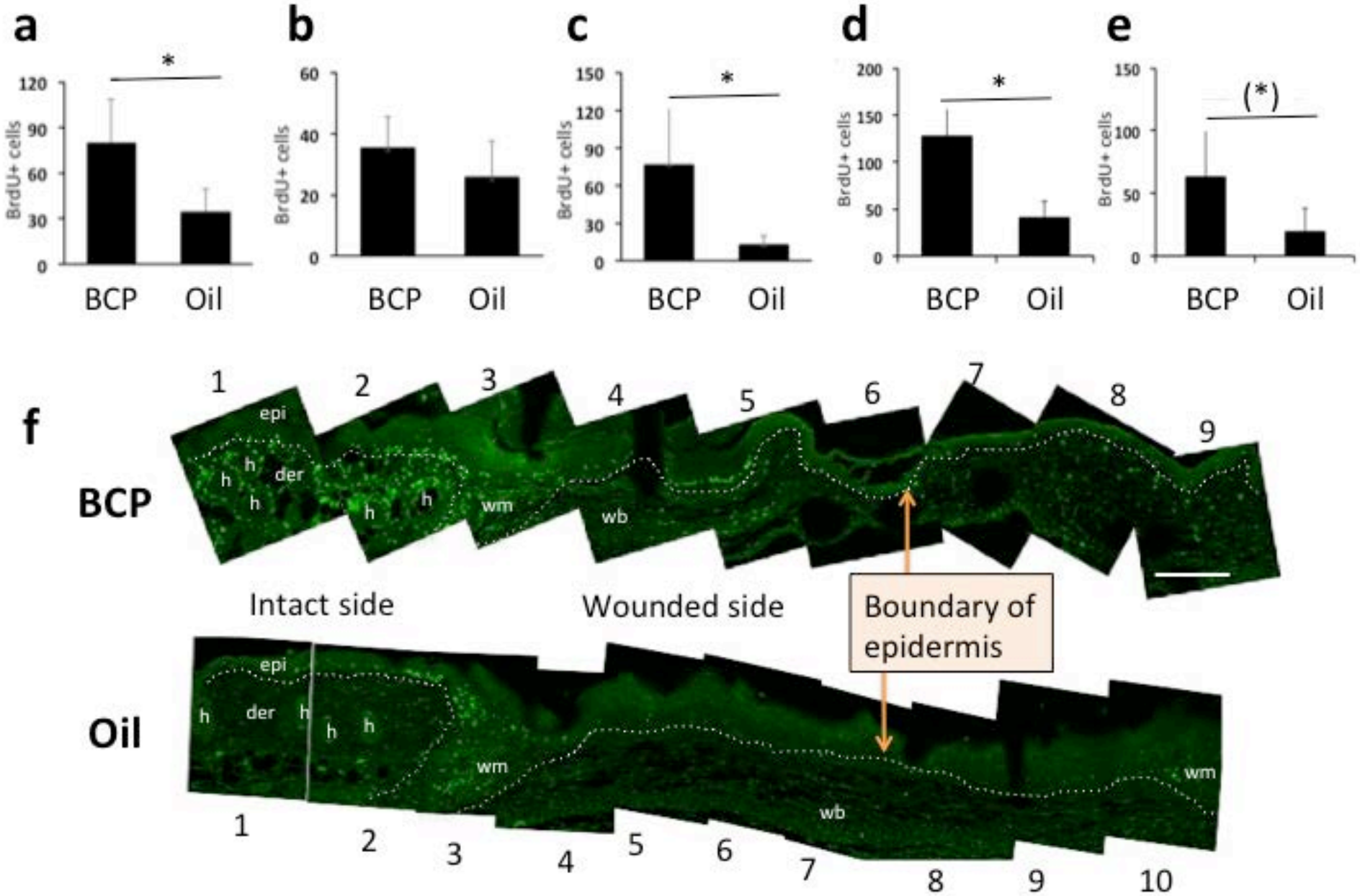
a
b
c
d
e
f
BrdU+ cells
BCP
Oil
*
(*)
BCP
Oil
epi
der
h
wm
wb
Intact side
Wounded side
Boundary of epidermis

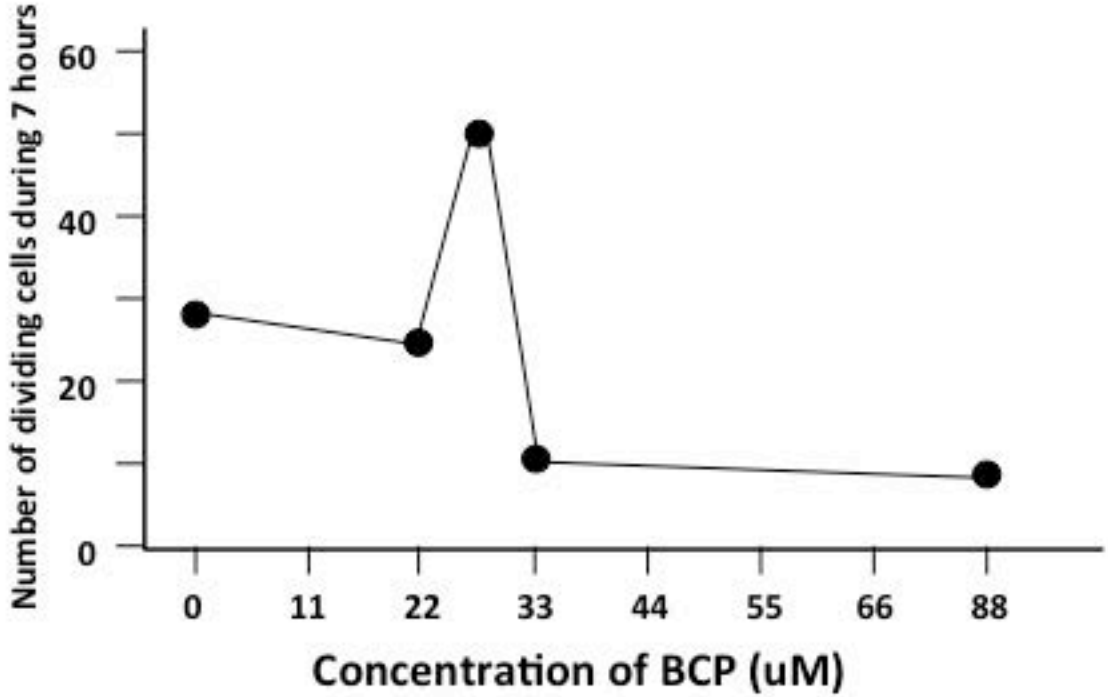
Number of dividing cells during 7 hours
60
40
20
0
0
11
22
33
44
55
66
88
Concentration of BCP (uM)

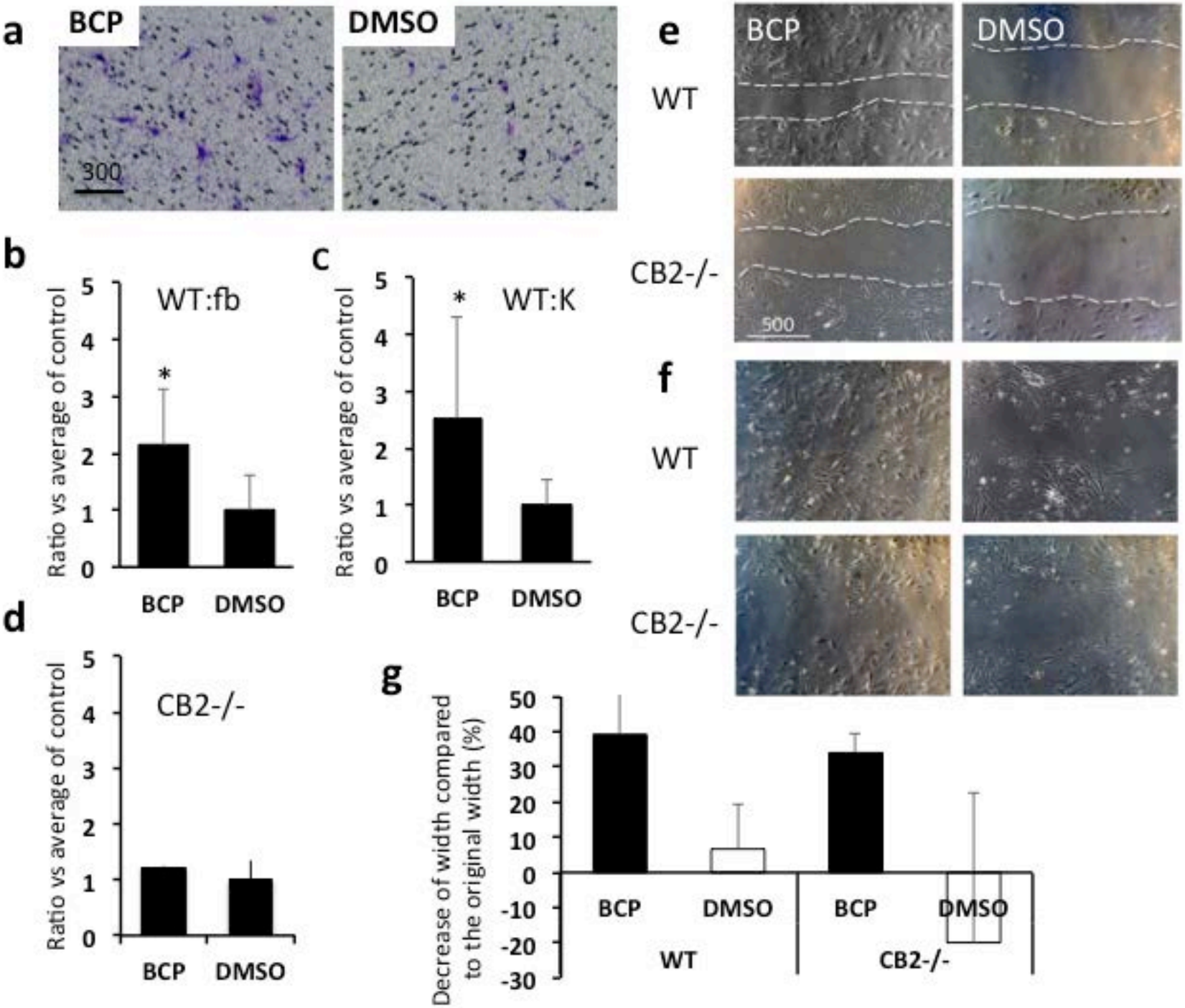
a
BCP
DMSO
300
b
WT:fb
Ratio vs average of control
BCP
DMSO
c
WT:K
Ratio vs average of control
BCP
DMSO
d
CB2-/-
Ratio vs average of control
BCP
DMSO
e
BCP
DMSO
WT
CB2-/-
500
f
WT
CB2-/-
g
Decrease of width compared to the original width (%)
BCP
DMSO
BCP
DMSO
WT
CB2-/-

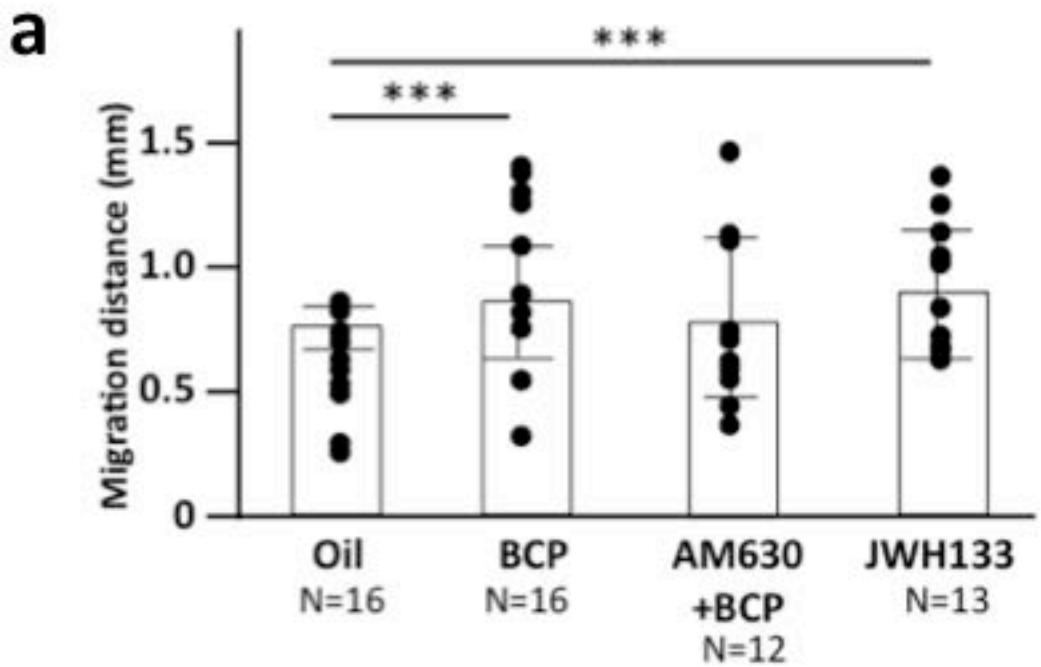
a
***
***
Migration distance (mm)
1.5
1.0
0.5
0
Oil
N=16
BCP
N=16
AM630
+BCP
N=12
JWH133
N=13

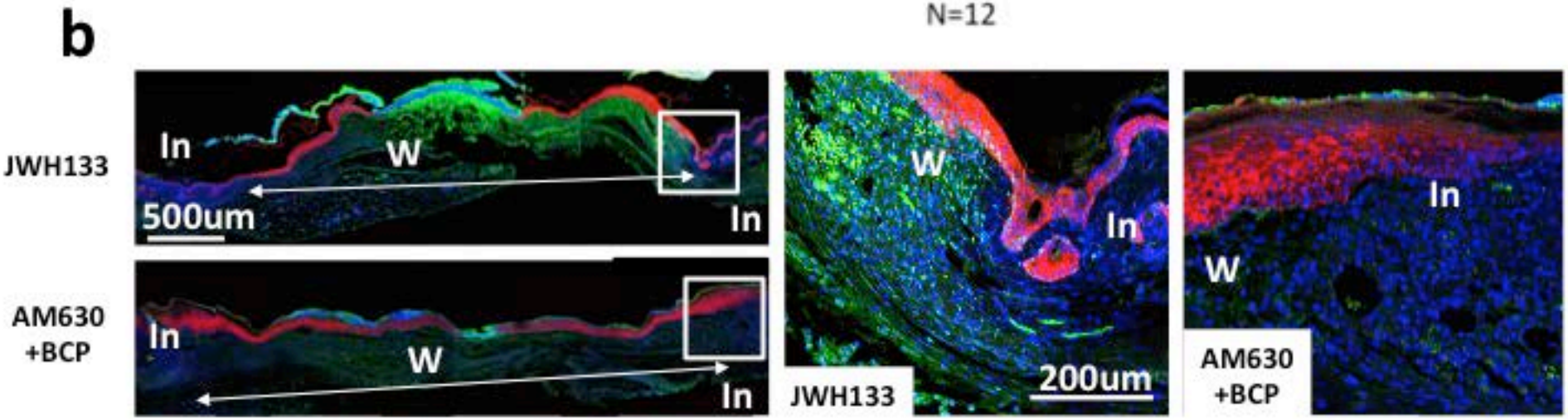
b
JWH133
In
W
500um
In
AM630
+BCP
In
W
In
W
In
200um
JWH133
In
W
AM630
+BCP

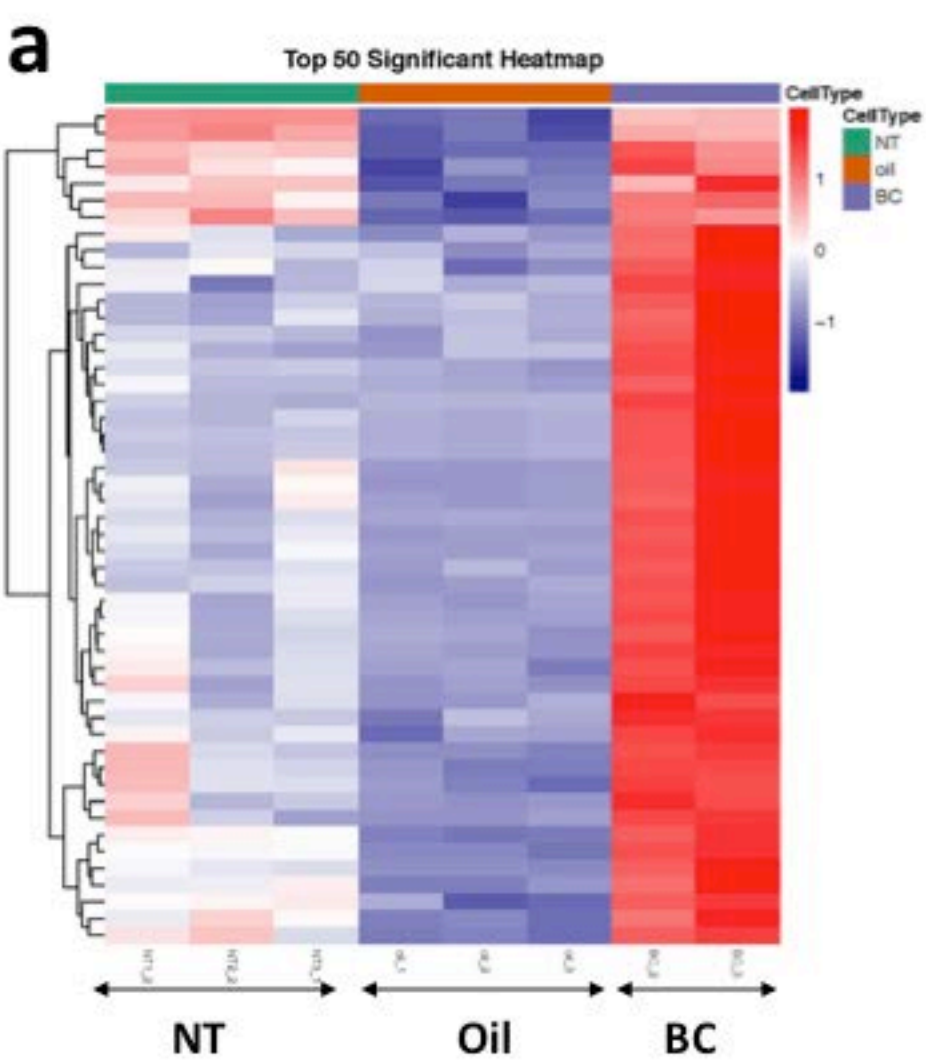
a
Top 50 Significant Heatmap
CellType
CellType
NT
oil
BC
1
0
-1
NT
Oil
BC

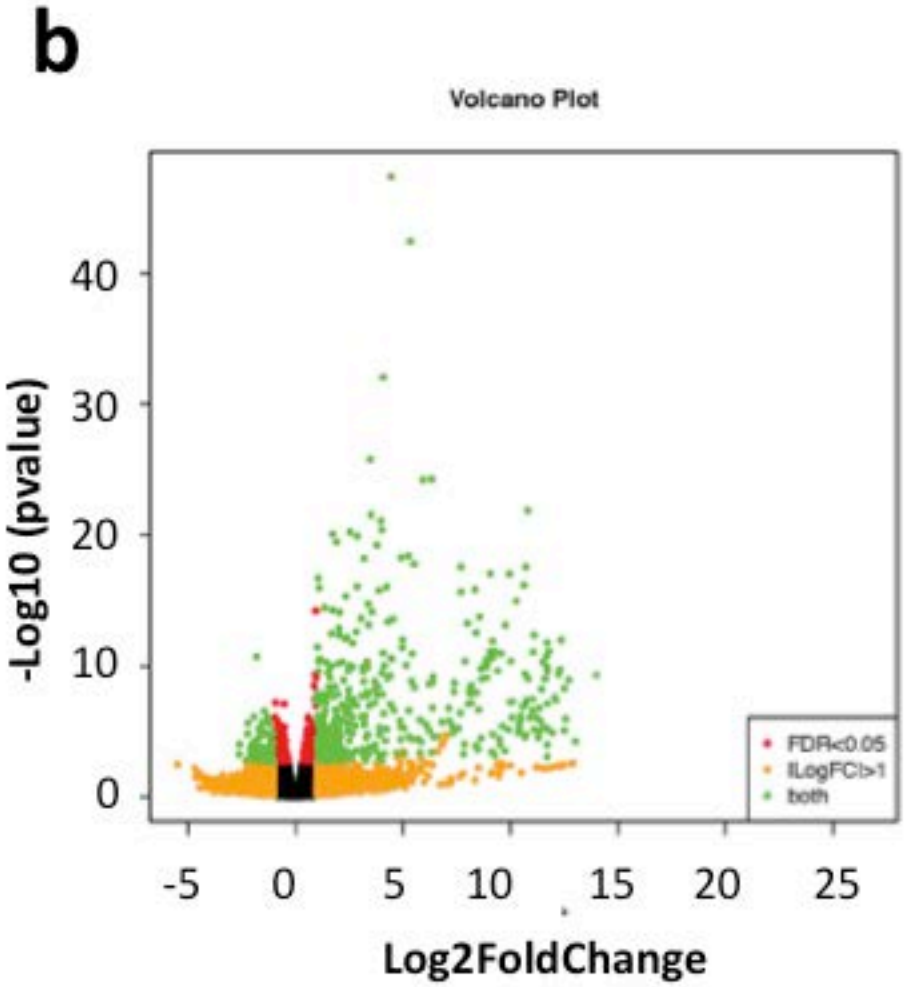
b
Volcano Plot
-Log10 (pvalue)
40
30
20
10
0
-5
0
5
10
15
20
25
Log2FoldChange
FDR<0.05
|LogFC|>1
both

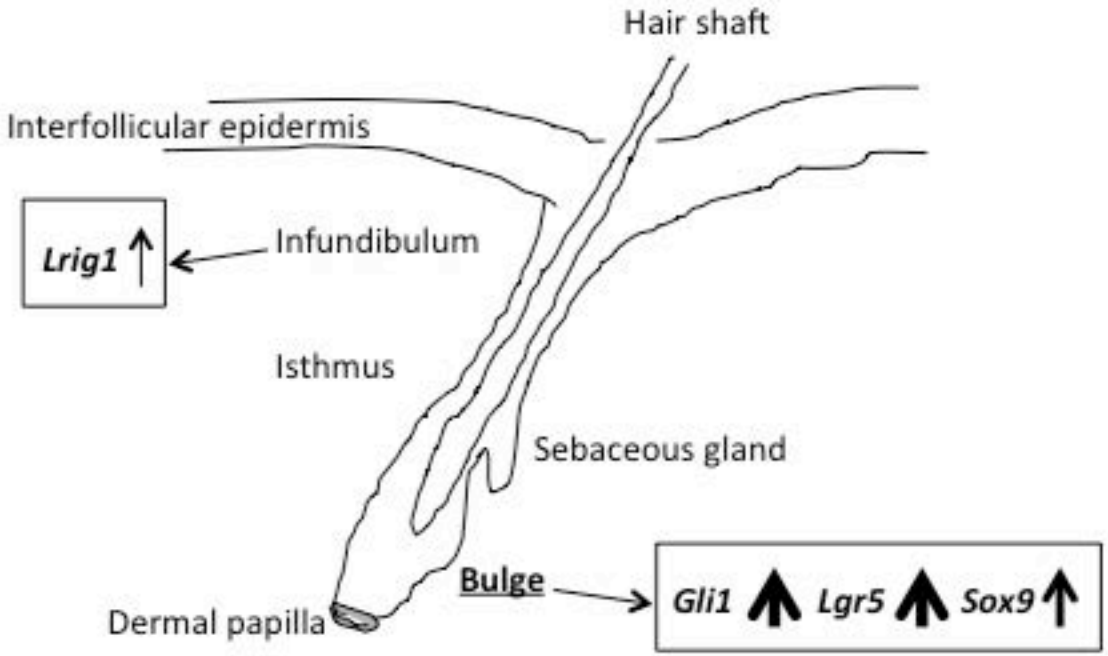

Expression of epidermal stem cell markers

Location	Gene	Logfoldchange	Pvalue	
interfollicular epidermis	*Lgr6*	0.384	0.08	
hair follicle Infundibulum	*Lrig1*	0.4035	0.013	*
	Plet1	-0.283	0.172	
isthmus	*Lgr6*	0.384	0.08	
bulge	*Gli1*	2.4605	1.76E-07	***
	Lgr5	1.236	0.001	***
	CD34	-0.199	0.454	
	Krt15	0.0646	0.71	
	Krt19	0.456	0.298	
	Sox9	0.5377	0.003	**
sebaceous gland duct	*Blimp1 (Prdu1)*	0.3291	0.081	

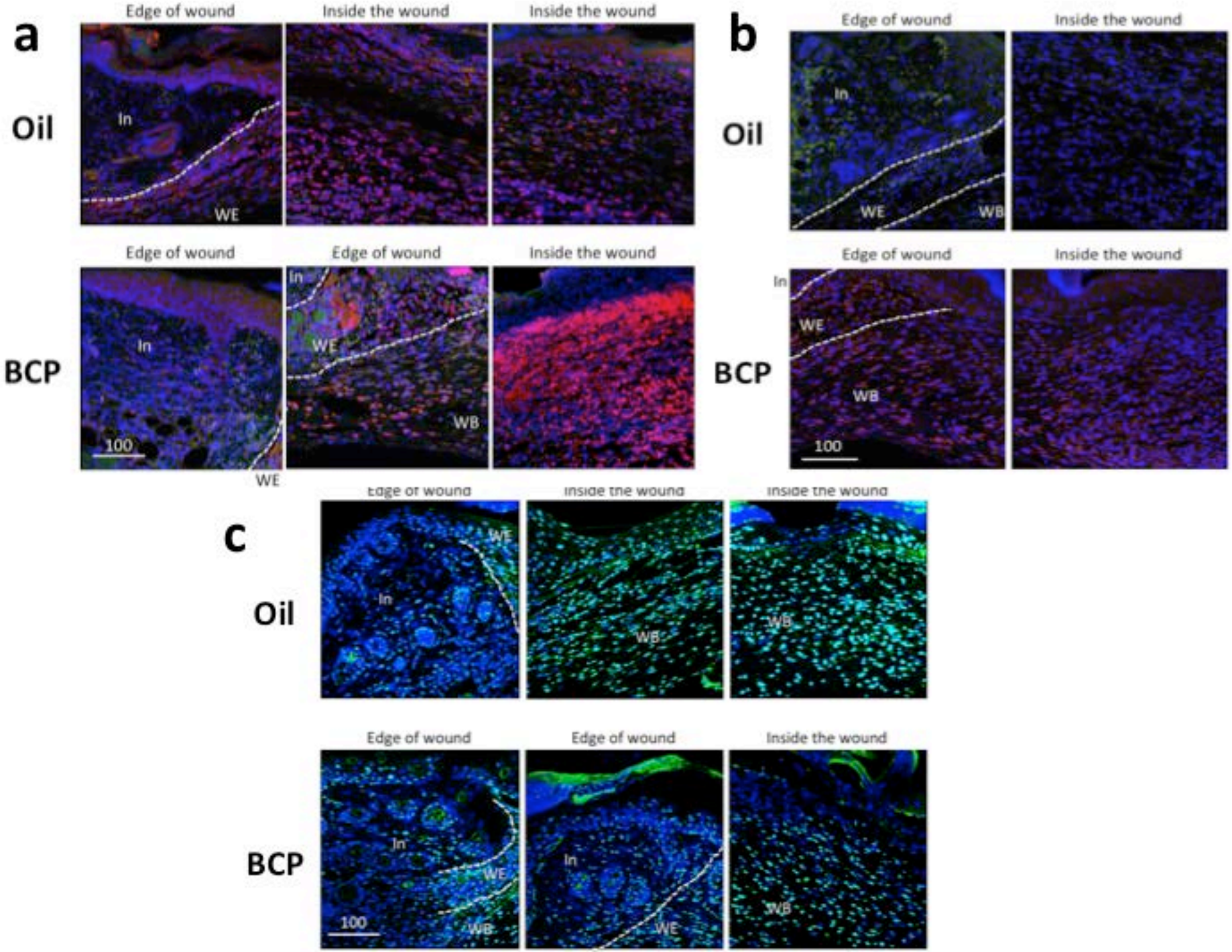
a
Oil
Edge of wound
Inside the wound
Inside the wound
In
WE
BCP
Edge of wound
Edge of wound
Inside the wound
In
WE
WB
100
b
Oil
Edge of wound
Inside the wound
In
WE
WB
BCP
Edge of wound
Inside the wound
In
WE
WB
100
c
Oil
Edge of wound
Inside the wound
Inside the wound
WE
In
WB
BCP
Edge of wound
Edge of wound
Inside the wound
In
WE
WB
100
In
WE
WB

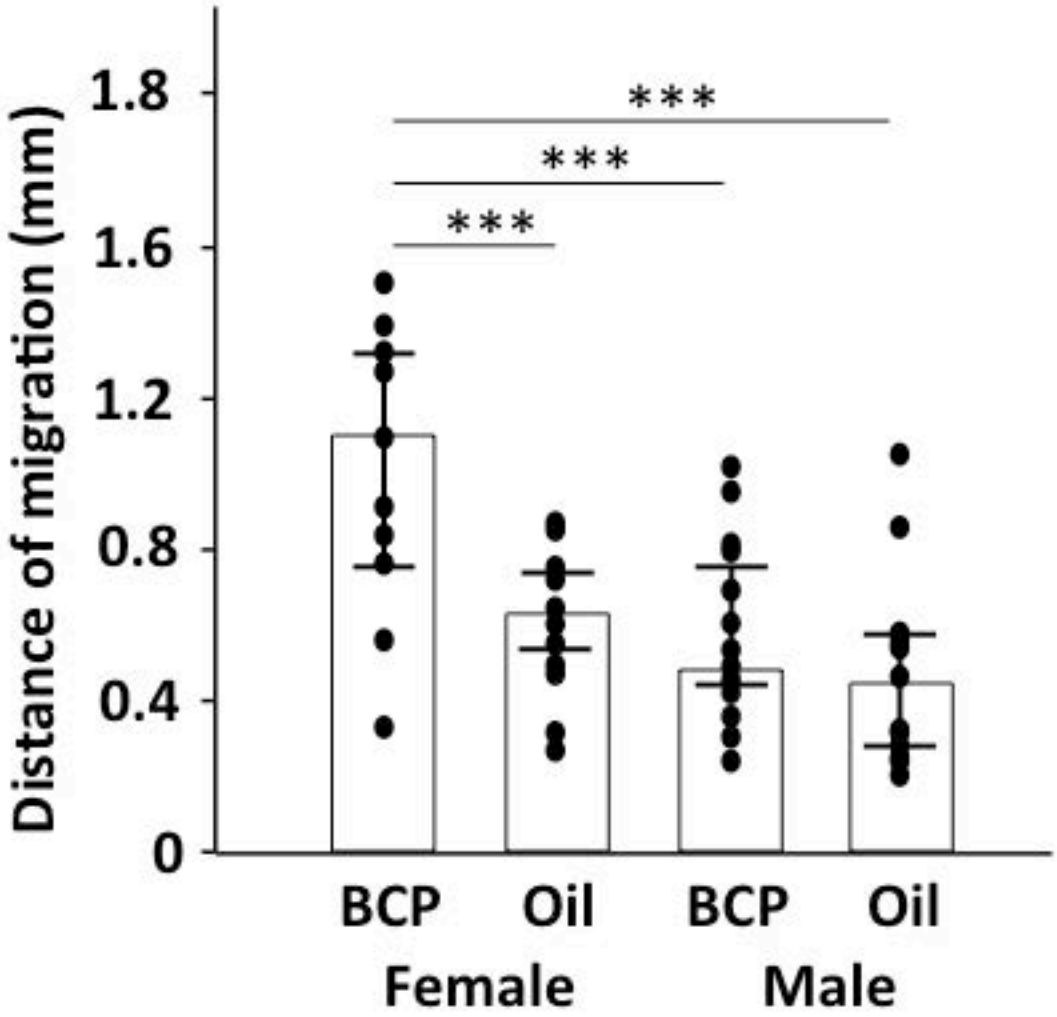
Distance of migration (mm)
1.8
1.6
1.2
0.8
0.4
0
***
***
***
BCP
Oil
BCP
Oil
Female
Male

Supporting information

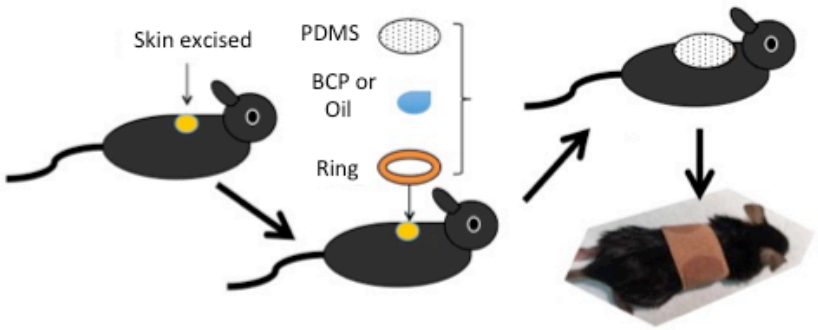

S1 Fig. Reservoir to hold treatment media. Small (5 mm x 5 mm) full-thickness excisions were made on the backs of adult mice and methods to hold the treatment buffer solution on the wounded area were developed. A silicone ring, which held 50 μL of buffer solution, was attached to the wounded area using a liquid sealing bandage (center). After the buffer solution was placed in the ring, a transparent lid made of polydimethylsiloxane (PDMS) was installed on top of the ring and was then sealed with the liquid sealing bandage (center and upper right). A gauze bandage was used to cover the body to prevent the mouse from removing the ring (lower right). (141 words)

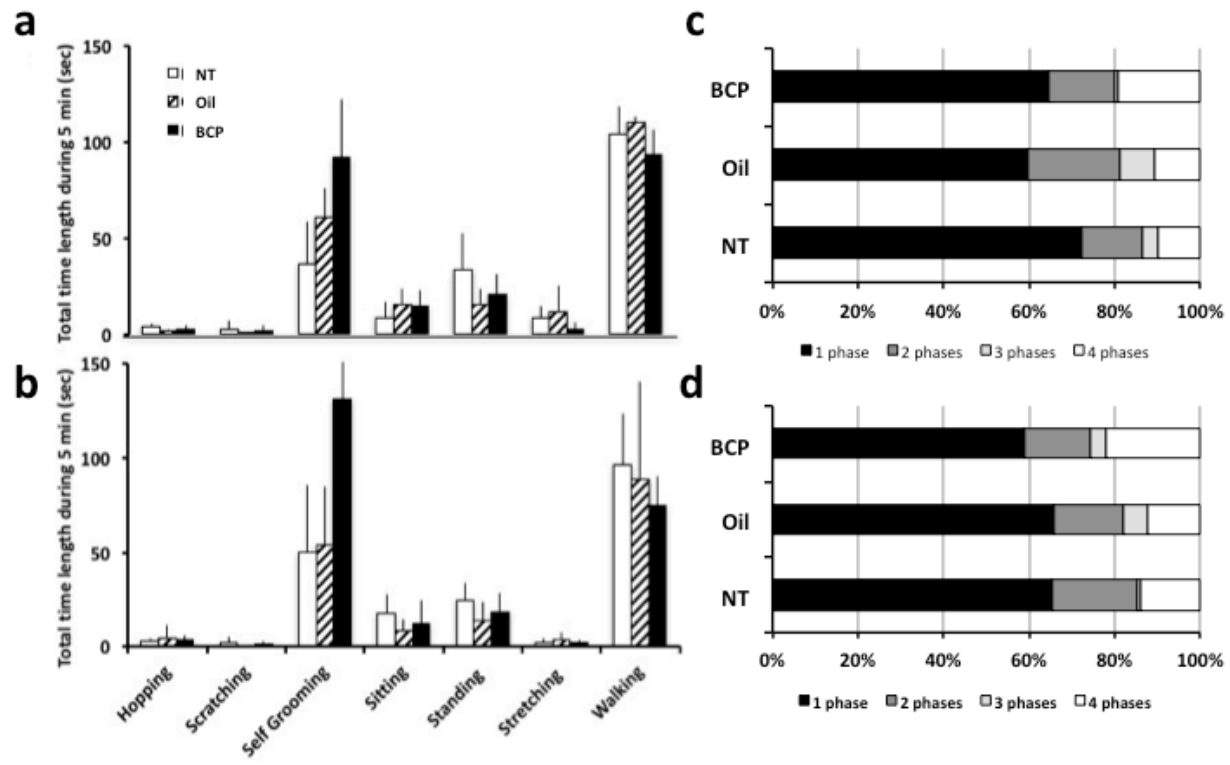

S2. Fig. Behavioral patterns observed by BCP, Oil, and NT group. A concern in the use of BCP is that it may cause allergic responses. An oxidation product of BCP, *i.e.*, caryophyllene oxide, is known as mild allergen [91]. To examine whether BCP has side effects, we conducted open-field tests on post-surgery day 1 (PS1) and 3 (PS3) and conducted behavioral analyses, specifically focusing on behavior patterns including scratching behaviors as an evidence of sensitization. In figures, NT group mice are mice without skin excision but went through all other steps and kept bandage on the same time length. There was almost no incidence of scratch behaviors on post-surgery day 1 **(a)** nor on post-surgery day 3 **(b)**. Statistically significant differences were found in self-grooming behaviors of post-surgery day 3 (ANOVA, $F_{2,15}$=4.585, P=0.028). Self-grooming behaviors

are known to increase at both high and low stress situations [92,93]. If there are differences in the way BCP group mice did self-grooming behaviors, it could be due to BCP treatment. We classified self-grooming behaviors by the part in the body they groom and called them Phase 1 to Phase 4 following earlier studies [92,93], and analyzed the self-grooming behaviors. We found no differences among the groups in the way self-grooming behaviors was conducted on both post-surgery day 1 and 3 (S2 Fig c,d), which suggest that BCP treatment did not cause mice to self-groom in a different way. **(c)** and **(d)** show the % of short to long, full sequences of self-grooming behaviors depending on the group on post-surgery day 1 **(c)** (NT, n=6, Oil, n=6, BCP, n=7) and 3 **(d)** (NT, n=6, Oil n=5, BCP, n=7). Classification of self-grooming behavior is as follows [92,93]: around the nose area (Phase I), around the face (Phase II), around the head and ears (Phase III), and to the body (Phase IV). Groomings toward the bandage were excluded from Phase IV to avoid the possibility that these grooming could be intention to remove bandages. Each incidence of grooming was classified into the number of phases they include and % of short self-groomings (include only one phase) to long full self-groomings (include four phases) were calculated to determine if BCP group showed shorter self-groomings as signs of irritation stress.
The % of self-grooming with four phases was higher in the BCP group but there were no statistically significant differences among groups. Based on these differences in the amount of self-grooming behaviors, we examined the travel distances and velocity of movements when they move and found that BCP group showed less travel distance and slower velocity (S3 Fig). (285 words)

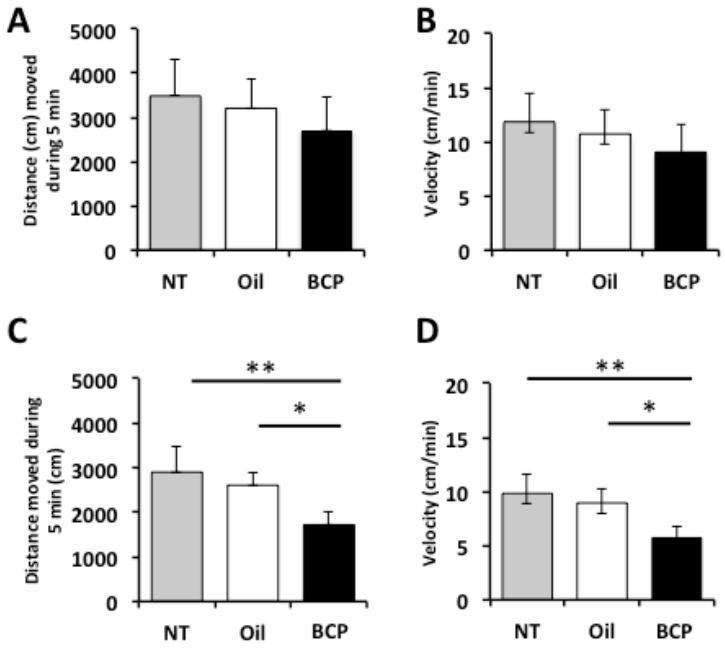

S3. Fig. Distance traveled and velocity of movements in BCP, Oil, and NT group mice. Open-field analyses of traveling distances and moving velocity revealed that on post-surgery day 1, there were no statistically significant differences among groups in the distance traveled **(a)** and velocity of movements **(b)** (ANOVA, distance, $F_{2,21}$=2.205, P=0.135; velocity, $F_{2,21}$=2.647, P=0.094; NT, n=6, Oil, n=6, BCP, n=7). On post-surgery day 3, the distance traveled **(c)** was significantly shorter and the velocity was significantly slower **(d)** in the BCP group, whereas there were no differences between the Oil group and NT group (ANOVA, distance, $F_{2,9}$=9.113, P=0.007; velocity, $F_{2,9}$=9.495, P=0.006; NT, n=6, Oil n=5, BCP, n=7). Linalool, a chemical compound included in lavender extracts, has anxiolytic effect in mice [68]. Whether the slower movements and increased self-grooming are signs that BCP has anxiolytic influence like linalool need to be addressed in future. Overall, these results

showed that the impact of BCP on behavior was the longer time staying at a place doing self-grooming and the slow movements when the mice walked, which contain no signs of irritation from allergic responses. The BCP we used contains only 1.6% of caryophyllene oxide (S4 Fig., S1 Table) and fresh BCP was applied daily. The daily change may have contributed to reduce sensitization and allergic reactions. (346 words)

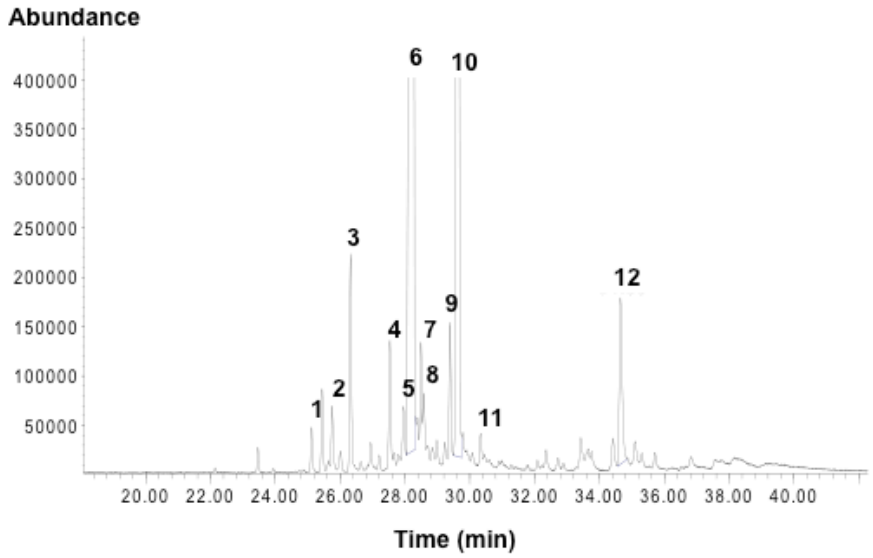

S4 Fig. Beta-caryophyllene standard (Sigma-Aldrich) composition/GC-MS. 1: cubebene, 2, 4, 5, 7, 8: sesquiterpenes of MW 204, 3: copaene, 6: BCP, 9: neoclovene, 10: α-caryophyllene, 11: 9-epi(E)-caryophyllene, 12: caryophyllene oxide. See **S2 Table** for details. (39 words)

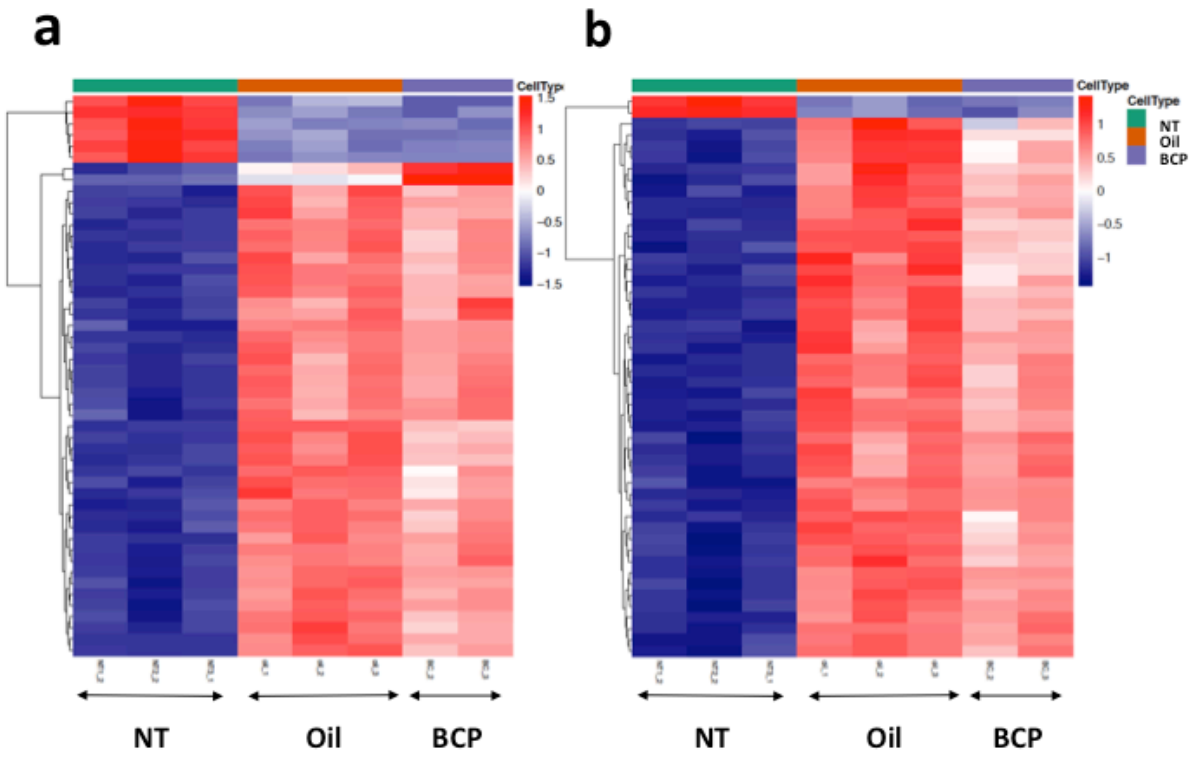

S5 Fig. Results of RNA sequencing of post-surgery 17 hours skin and intact skin: Comparison between BCP and NT (a) and Oil and NT (b). Heatmap showing the top 50 significant gene expressions in the skin exposed to BCP (n=2) or oil (n=3), 17 to 18 hours post-surgery (inflammation stage), and in the skin of mice without skin excision (NT group) (n=3).

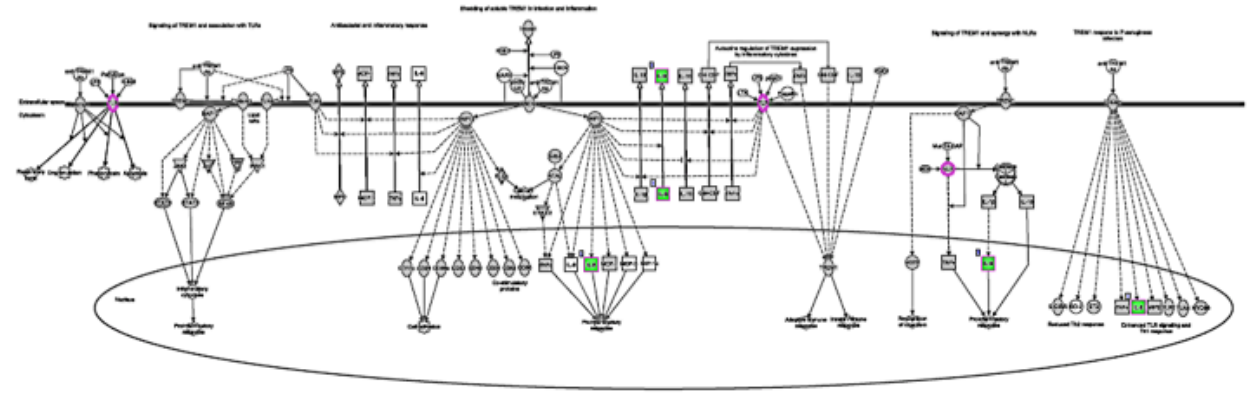

S6 Fig. Influence of exposure to BCP on TREM1 pathway. TREM1 signaling pathway showing the genes/groups of genes up-regulated (pink) and down-regulated (green) in BCP group compared to oil group. (28 words)

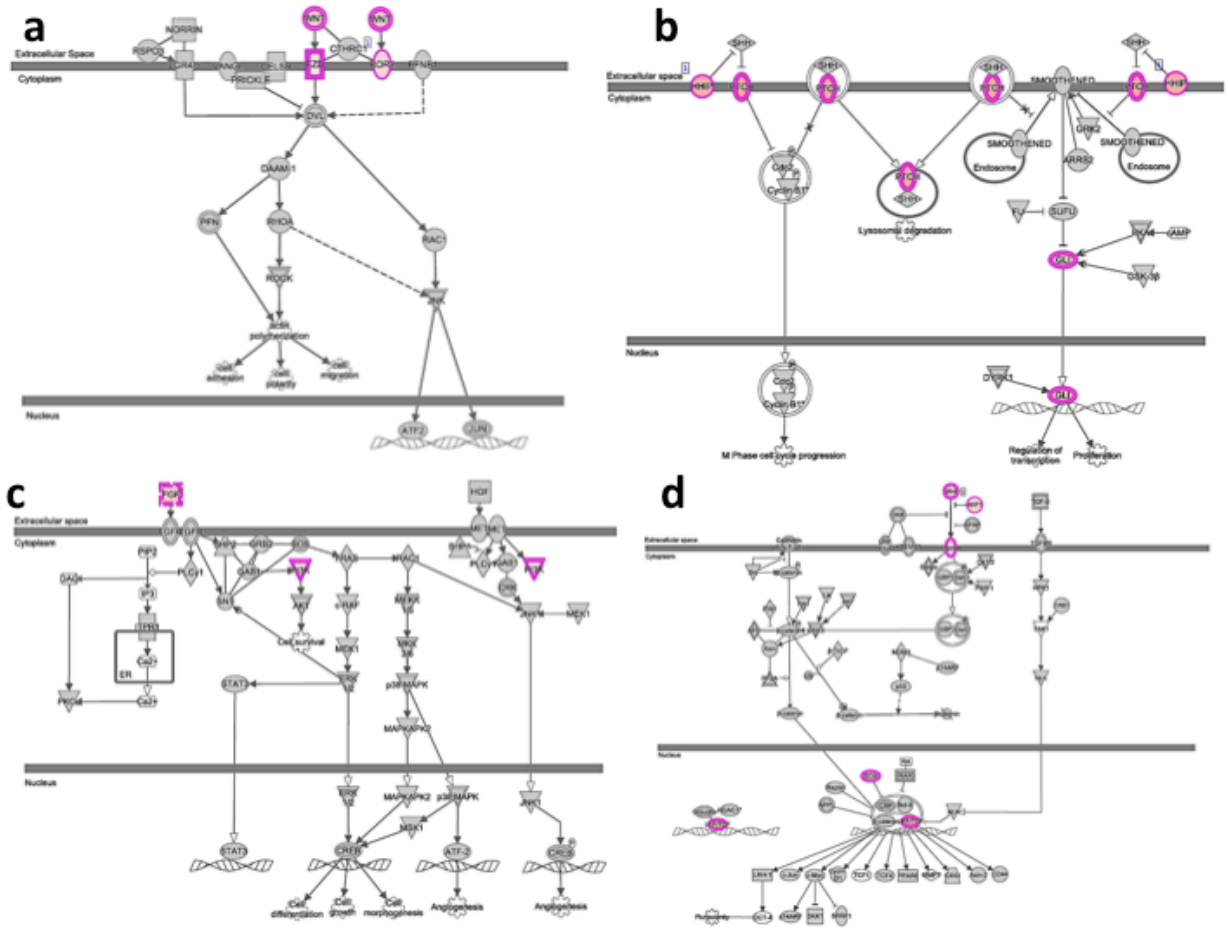

S7 Fig. Signaling pathways showing the genes/groups of genes up-regulated (pink) in BCP group compared to oil group... **(a)** Sonic hedgehog signaling (shh) pathway, **(b)** planar cell polarity (PCP) signaling pathway, **(c)** fibroblast growth factor (FGF) signaling pathway, and **(d)** Wnt beta-catenin signaling pathway. (42 words)

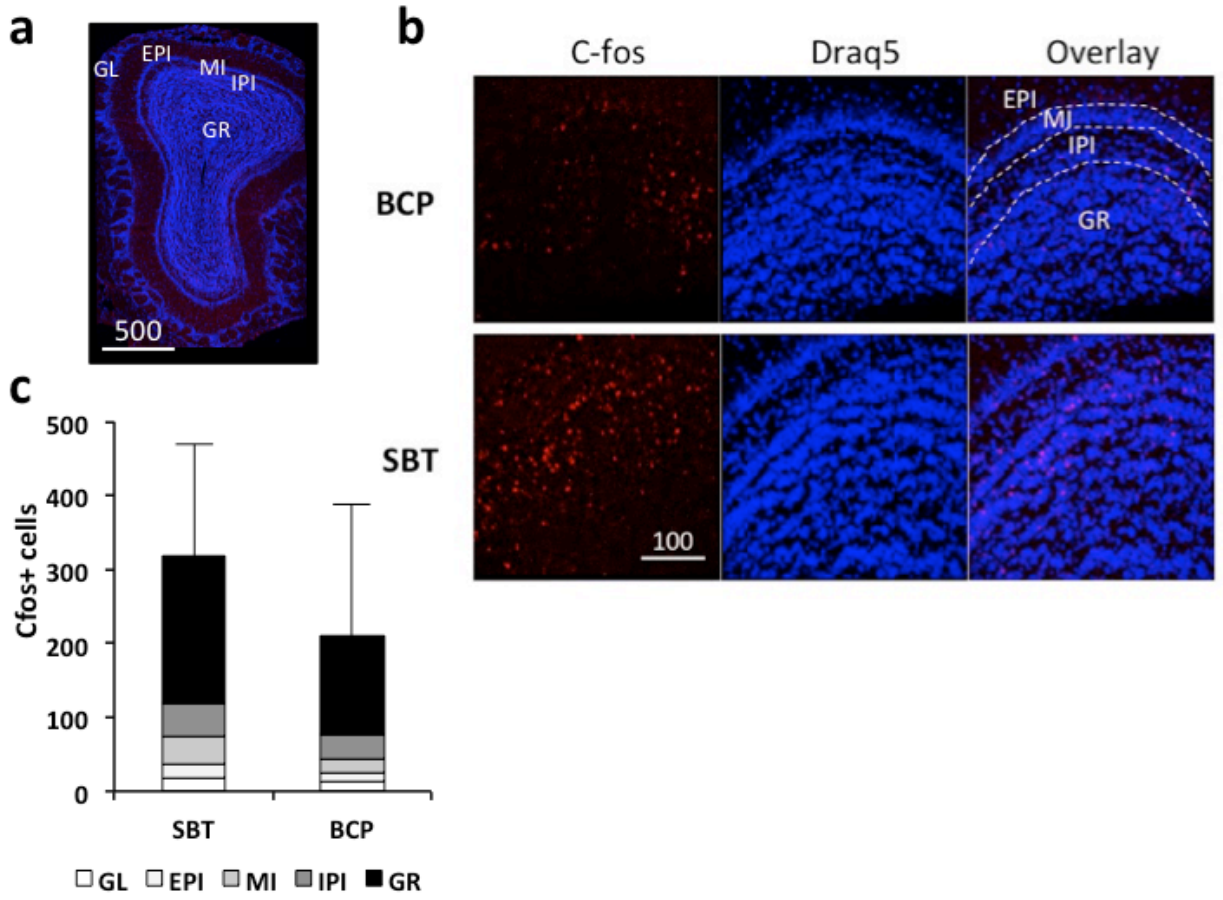

S8 Fig. cfos expression in the olfactory bulb of mice exposed to BCP or SBT. (a) Location where cfos was expressed profoundly. B **(b)** To test if mice can smell BCP, intact mice were exposed to BCP (n=3) or male murine pheromone 2-sec-butyl-4,5-dihydrothiazole (SBT) (n=5) [61,62] for 60 min and perfused. Olfactory bulb was harvested, and processed to determine c-fos protein expression. Mice exposed to BCP and SBT both showed c-fos expression in the olfactory bulb. **(c)** Numbers of cfos+ cells were not statistically significantly different between the mice exposed to SBT and BCP because of the large variance in the expression of cfos. The expression was high in the females at estrous stage. Error bars indicates sd of total number of cells. GL: glomerular layer, EPI: external

plexiform layer, MI: mitral cell layer, IPI: internal plexiform layer, GR: granule cell layer.

(141 words)

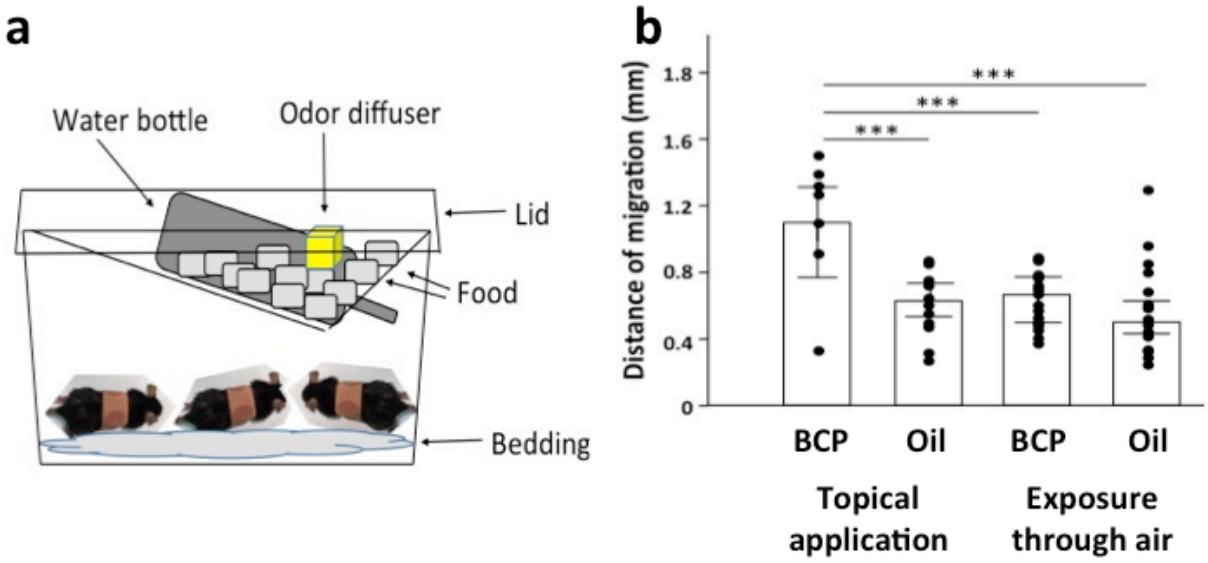

S9 Fig. Influence of exposure to BCP through the olfactory system. Mice were exposed to BCP or olive oil (Oil) through air by putting Q-tip soaked with either BCP or olive oil in a wire mesh and placing the wire mesh on top of the food provider **(a)**. Food was placed as much as possible to avoid the possibility that mice can reach to the wire mesh. Mice went through surgery and surgery area was covered by the ring reservoir filled with olive oil and sealed by PDMS lid, which was covered by a bandage. **(b)** Exposure to BCP through air did not differ from control level and significantly different from topical application of BCP (ANOVA, BCP vs Oil $F_{1,66}=15.803$, $P<0.001$, Topical vs Air $F_{1,66}=13.01$, $P=0.001$, Interaction $F_{1,66}=6.701$, $P=0.012$, BCP-Top, n=16, Oil-Top, n=16, BCP-Air, n=18, Oil-Air,

n=20) ***: P<0.001, Tukey's pairwise comparison was used for pair wise comparison. (138 words)

S1 Table. Beta-caryophyllene standard (W225207, Sigma-Aldrich) composition/GC-MS

No. in S4 Fig.	Rt (min)	Peak area x 10^6	Compound	%
1	25.11	0.831	Cubebene	0.1
2	25.75	1.379	a sesquiterpene, MW 204	0.2
3	26.31	5.299	Copaene	0.8
4	27.52	3.308	a sesquiterpene, MW 204	0.5
5	27.95	1.198	a sesquiterpene, MW 204	0.2
6	28.21	546.676	β-caryophyllene	81.8
7	28.49	1.704	a sesquiterpene, MW 204	0.3
8	28.59	0.4799	a sesquiterpene, MW 204	0.1
9	29.38	2.659	neoclovene	0.4
10	29.63	93.877	α-caryophyllene	14.0
11	20.33	0.681	9-epi(E)-caryophyllene	0.1
12	34.63	10.416	caryophyllene oxide	1.6
	SUM	668.508		100.0

S2 **Table. Olfactory receptor genes in the olfactory epithelium up-regulated after 1 hour exposure to BCP**

Olfactory Receptor Gene	Log2FC	PValue
Olfr340	4.892	0.005
Olfr1480	1.881	0.028
Olfr103	1.656	0.001
Olfr1054	1.469	0.028
Olfr44	1.425	0.001
Olfr935	1.382	0.016
Olfr1152	1.325	0.041
Olfr616	1.246	0.037
Olfr1356	1.138	0.035
Olfr508	1.124	0.048
Olfr111	1.066	0.021
Olfr1258	1.013	0.002
Olfr33	0.928	0.042
Olfr874	0.880	0.026
Olfr599	0.810	0.022
Olfr92	0.780	0.046
Olfr716	0.736	0.015
Olfr701	0.729	0.048
Olfr1427	0.687	0.039

S3 Table. Olfactory receptors expressed in skin after exposure to BCP, compared with Oil group

Olfactory receptor genes	Log2FC	Pvalue
Olfr267	2.575	0.355
Olfr624	1.336	0.544
Olfr912	0.497	0.661
Olfr1396	0.378	0.796
Olfr1034	0.344	0.859
Olfr110	0.256	0.780
Olfr212	0.211	0.925
Olfr482	0.075	0.737
Olfr558	-0.115	0.788
Olfr920	-0.14	0.777
Olfr1392	-0.151	0.965
Olfr750	-0.222	0.937
Olfr733	-0.243	0.929
Olfr78	-0.249	0.683
Olfr523	-0.279	0.862
Olfr560	-0.296	0.871
Olfr77	-0.466	0.668
Olfr346	-0.81	0.714
Olfr56	-0.836	0.264
Olfr466	-0.847	0.588
Olfr1378	-0.853	0.636
Olfr92	-0.883	0.604
Olfr1033	-0.898	0.221
Olfr111	-1.06	0.134
Olfr1383	-1.324	0.613
Olfr1388	-1.376	0.451
Olfr433	-1.806	0.405
Olfr1393	-2.218	0.395
Olfr432	-2.707	0.440
Olfr1564	-2.74	0.265